Reaction studies from below to well above the Coulomb Barrier energies



Dr. Kavita Rani Post-Doctoral Fellow, ICARE Group, HIL

Research Experience

2015 - 2021 Doctor of Philosophy

Experimental Nuclear Physics - Low energy nuclear reactions
DST-INSPIRE FELLOW, Cyclotron lab
Panjab University, Chandigarh, INDIA-160014





अंतर विश्वविद्यालय त्वरक केंद्र Inter-University Accelerator Centre - (IUAC)

2022 -2024 Post Doctoral research associate

Experimental Nuclear Physics – Study of Fission Dynamics Nuclear Reaction Group, Variable Energy Cyclotron Centre Kolkata, INDIA-700064 Government of India
Department of Atomic Energy
VARIABLE ENERGY CYCLOTRON CENTRE

EXPERIMENTS

Fusion

- Barrier distributions, ER cross section experiments, etc
- Transfer reactions and their angular distributions

Fission

- Mass distributions, Angular Distributions
- Mass gated Neutron multiplicity, Charge Particle multiplicity

Barrier Distribution

Mass distributions

Mass gated Neutron multiplicity

RESEARCH MOTIVATION

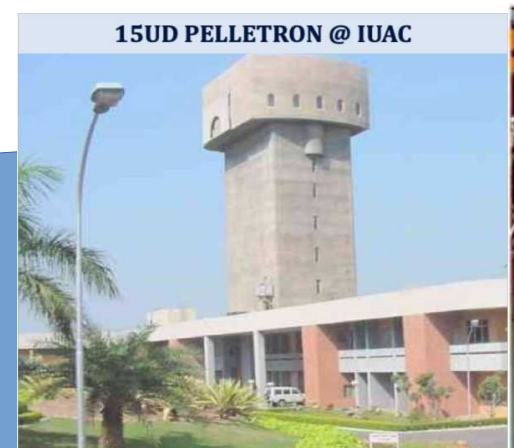
Heavy-Ion fusion-fission reactions

- -> nuclear astrophysics
- -> energy generation in the stellar environment
- -> production of exotic nuclei
- -> synthesis of SHE
- -> data to reach optimized irradiation conditions for the development of next generation nuclear reactors

Heavy-Ion peripheral reactions

- -> QEL potential parameters for different nuclear reactions
- ICF and transfer a promising spectroscopic tool to achieve high spin states
- -> provide a sensitive probe for nuclear structure studies

Sets of experiments were performed at Inter-University Accelerator Centre (IUAC), New Delhi and Variable Energy Cyclotron Centre (VECC), Kolkata



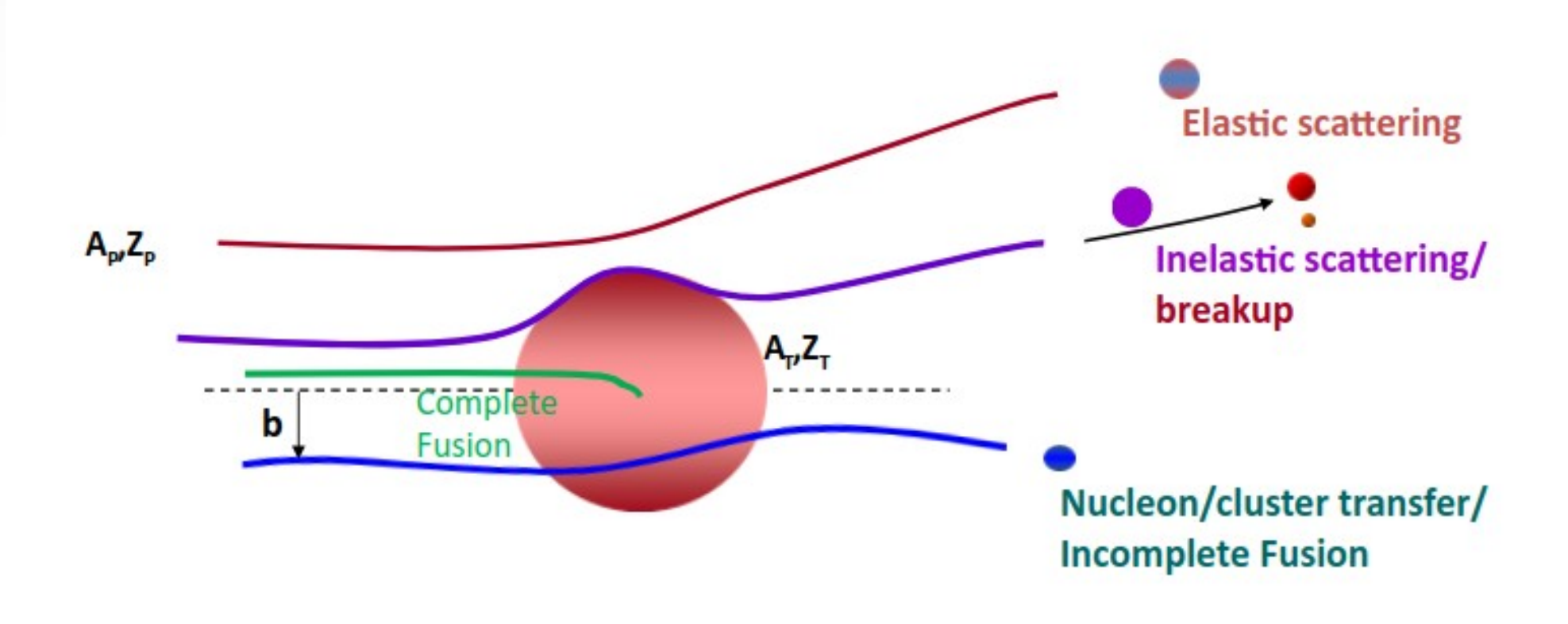


OUTLINE

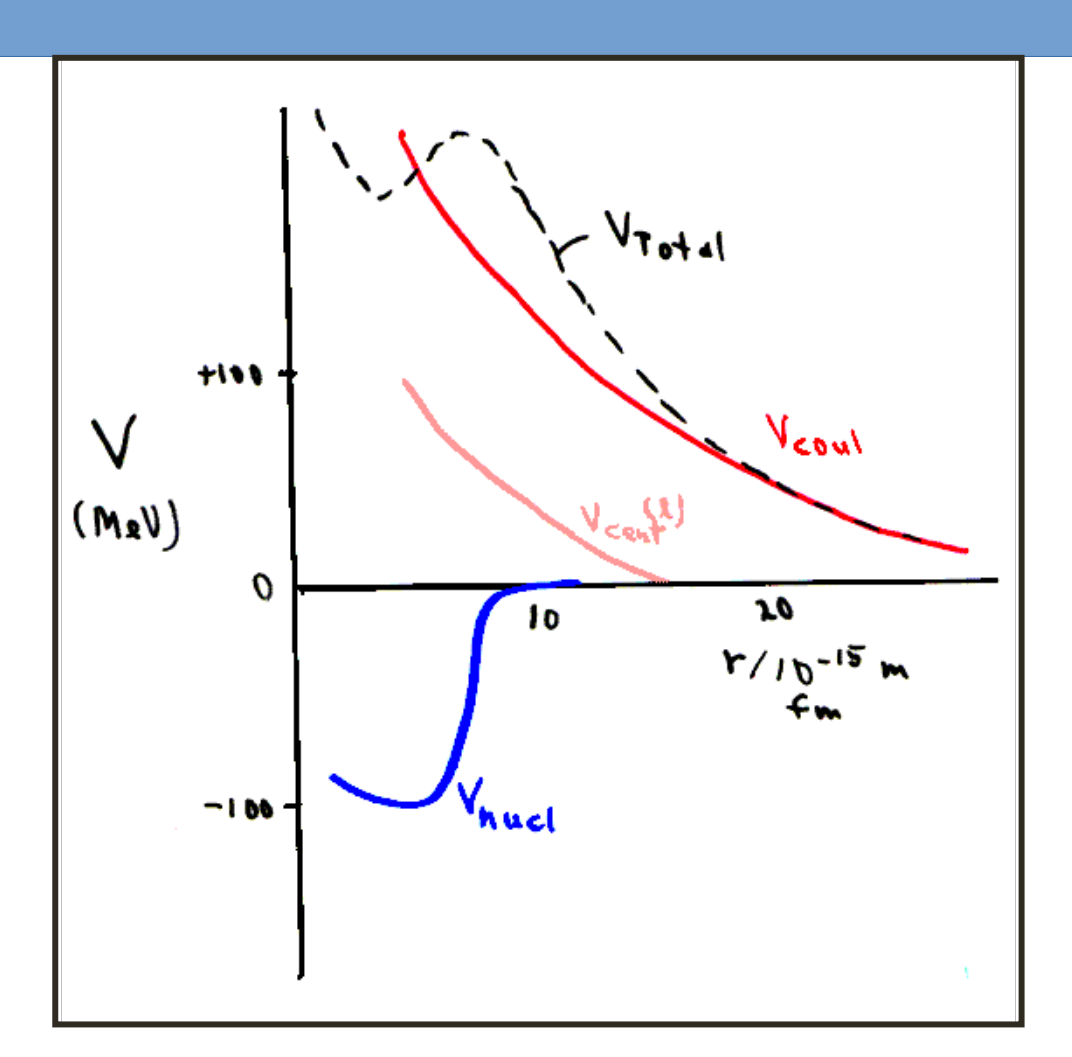
- ◆ Quasi-elastic Measurements for ²⁸Si+¹⁴⁴Sm
- Fusion-Fission Dynamics at wide excitation energy range
- Neutron Multiplicity Measurements for α + ²³²Th reaction

Quasi-elastic Measurements for ²⁸Si+¹⁴⁴Sm

Reaction Channels Around the Coulomb Barrier



Inter-nucleus potential



Three forces:

- 1. Coulomb force
- 2.Centrifugal force

Long range, repulsive

3. Nuclear force Short range, attractive



Potential barrier due to the compensation between the three

$$V_{total} = V_c + V_n + V_{cent}$$

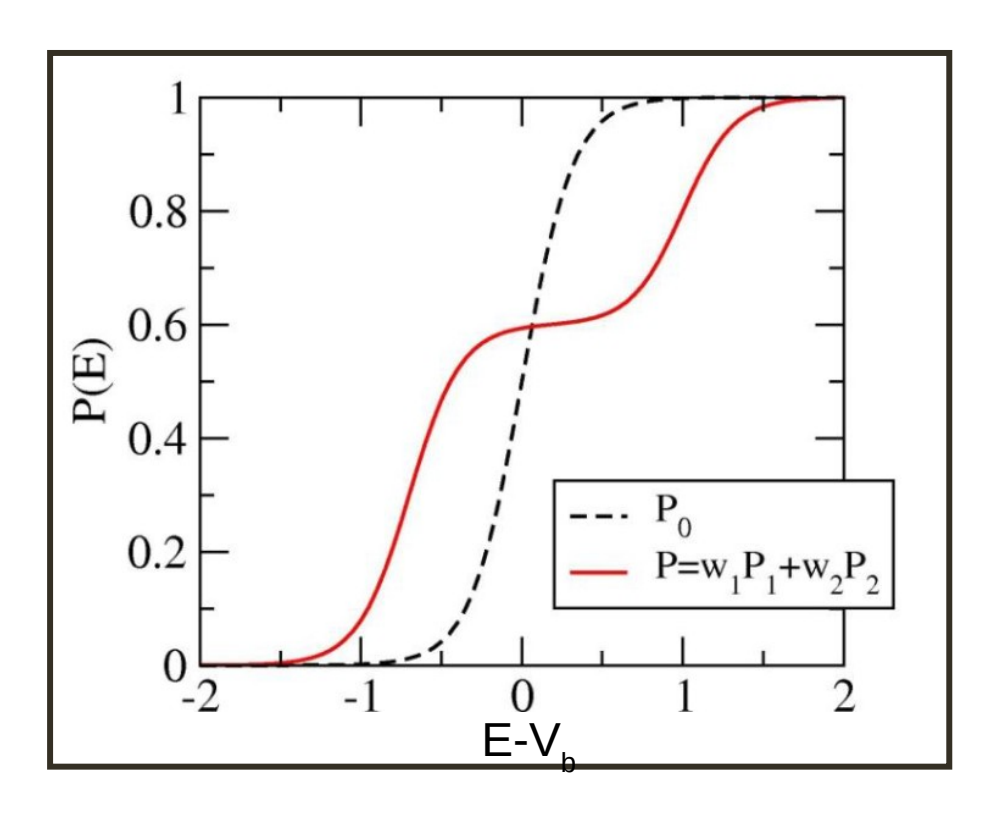
Classically fusion is possible only when E > V_b

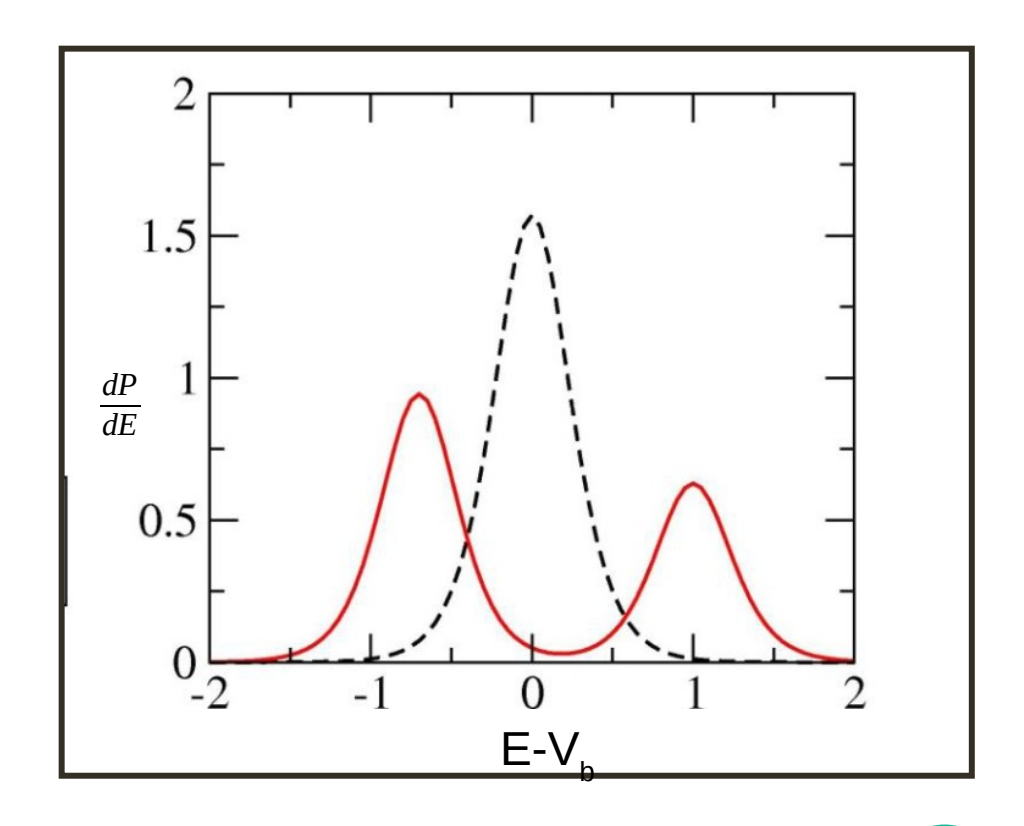
$$\sigma_{\mathsf{fus}}^{cl}(E) = \pi R_b^2 \left(1 - \frac{V_b}{E} \right)$$

TUNNELING EFFECT

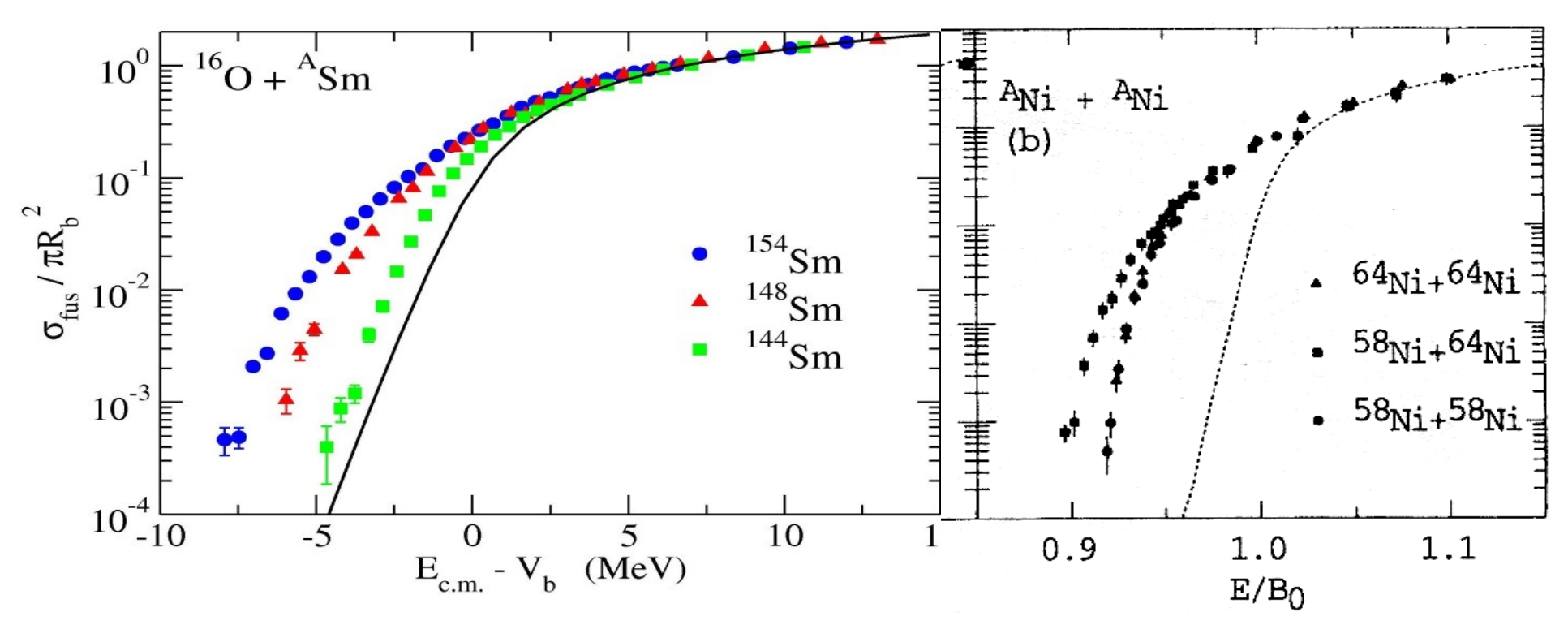
But Fusion takes place by quantum tunneling at low energies

$$\sigma_{\mathsf{fus}}(E) = \frac{\pi}{k^2} \sum_{l} (2l+1) P_l(E)$$





Experimental Discrepancies



One dimensional Penetration model successfully explains experimental observations for $E>V_b$ but fails to explain the experimental results at $E<V_b$.

¹⁵⁴Sm is highly deformed. The height of the barrier depends on its orientation.

The Q-value for transfer in reaction ⁵⁸Ni+⁶⁴Ni has positive values which was used to account for the discrepancies from One-D Penetration Model.

Barrier Distribution

- Coupling to other channels during the fusion reaction, splits the potential barrier into a number of barrier. This distribution obtained due to coupling s termed as barrier distribution (BD).
- Fusion Barrier Distribution can be experimentally obtained from the double derivative of the product of projectile energy and experimental fusion cross-section.

 $D_{\mathsf{fus}}(E) \equiv \frac{d^2(E\sigma_{\mathsf{fus}})}{dE^2} \simeq \pi R_b^2 \frac{dP_{l=0}}{dE}$

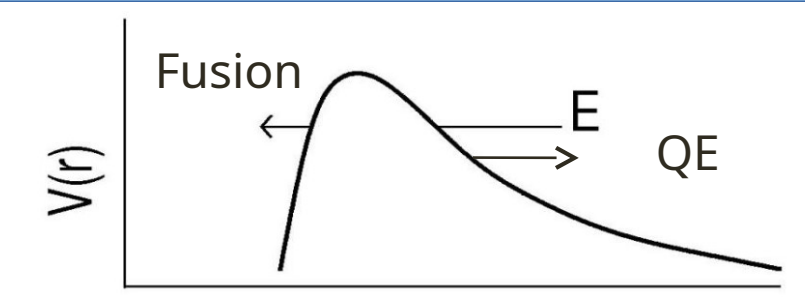
BD is considered to be better tool to study the reaction dynamics as it is obtained from the derivative of the cross-section. Any small change in the cross-section will bring a bigger change in the shape of the distribution.

N. Rowley, G.R. Satchler, P.H. Stelson, PLB254("91)25

Quasi-Elastic Scattering and Quantum Reflection

In quantum mechanics, reflection occurs even at *E* > *Vb i.e.* Quantum Reflection

$$P(E) + R(E) = 1$$



Reflection prob. carries the same information as penetrability, and barrier distribution can be defined in terms of reflection prob.

A sum of all the reaction processes other than fusion (elastic + inelastic + transfer +)

Detect all the particles which reflect at the barrier and hit the detector

Related to reflection and Complementary to fusion

Quasi-elastic barrier distribution

$$D_{\mathsf{qel}}(E) = -rac{d}{dE} \left(rac{\sigma_{\mathsf{qel}}(E, \pi)}{\sigma_R(E, \pi)}
ight)$$

M.V.Andres et al., Phys. Lett. B,1988 H. Timmers et al., NPA584("95)190

Advantages for D_{qel}

- Less statistical error in QE (1st vs. 2nd derivative)
 - Much easier to be measured

Qel: a sum of everything

a very simple charged-particle detector

Fusion: requires a specialized recoil separator to separate ER

ER + fission for heavy systems

Several effective energies can be measured at a single-beam energy

$$E_{\text{eff}} = 2E \sin(\theta/2)/[1 + \sin(\theta/2)]$$

Extraction of BD theoretically

- Theoretically, the coupled channels calculations are performed to obtain the fusion/QE cross-section and then using the point difference formula to find the second derivative for obtaining the BD.
- Various codes are available to perform these calculations. These codes include CCDEF,
 CCFUS, CCFULL.
- CCFULL is employed for the study of fusion. This code takes into consideration the vibrational, rotational nature of the target and projectile into consideration and to a few extent, this code includes only pair transfer.
- For Quasi-elastic scattering, the scattering version of CCFULL i.e CCQUEL is employed. This code gives us the QE excitation function and taking its first derivative w.r.t energy gives us the barrier distribution.
- The details of the inputs to be given in these codes will be discussed later.

C.H. Dasso et alnComputer Phys. Commun. 46, 187 (1987). J. Fernandez-Niello et al Computer Phys. Commun. 54, 409 (1989).

K. Hagino, et al, Comput. Phys. Commun. 123, 143 (1999)

K. Hagino, yet to published..

QE Measurements: 28Si+144Sm; Why interesting??

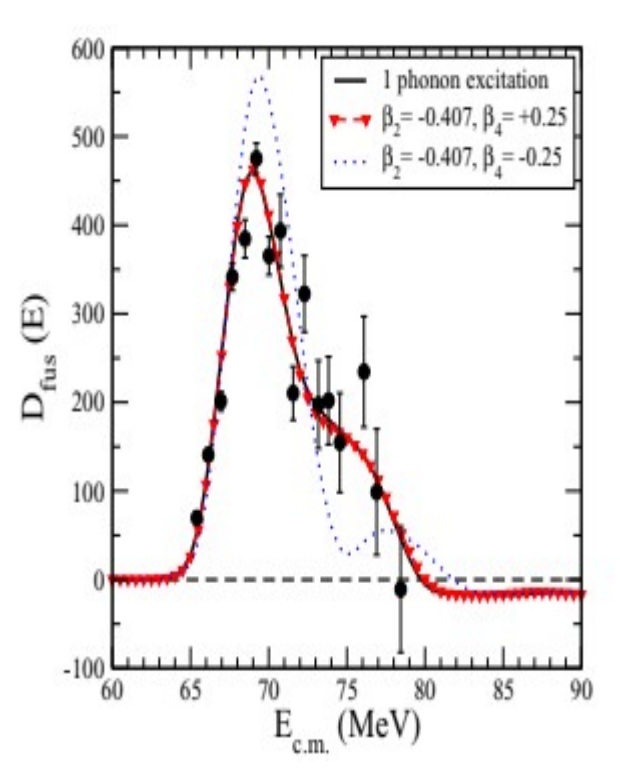
- Role of target excitations on fusion has been widely studied.
- Various fusion studies has shown ²⁸Si as both vibrator as well as rotor.
- For studying the target structural effect, there are number of QE-studies but only few for the study of projectile excitations.
- These are the recent studies which includes ²⁸Si as projectile and are for the systems ²⁸Si+¹⁵⁴Sm, ^{142,150}Nd, ⁹⁰Zr.

QE Measurements: 28Si+144Sm; Why interesting??

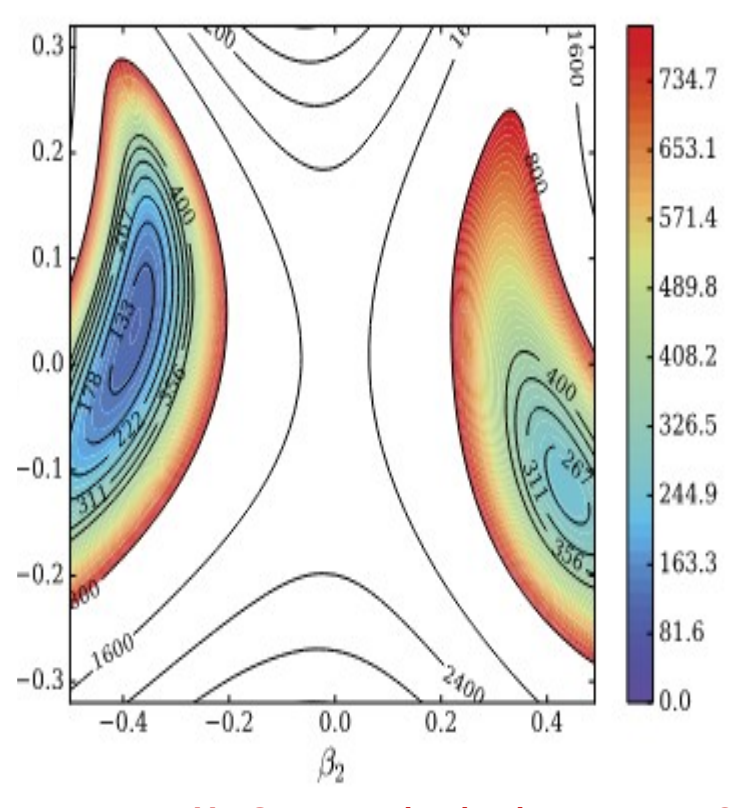
Wide range of determined hexadecupole deformation of ²⁸Si Insight into projectile structure role on the quasi-elastic barrier distribution(QE-BD)

•		
Experiment	β_2	β_4
Present work	-0.38 ± 0.01	+0.03±0.01
$(CE^1)[27]$	-0.39	
(e, e') [26]	-0.39	+0.10
(n, n') [28]	-0.39	
(n, n') [42]	-0.48	0.15
(n, n') [42]	-0.42 ± 0.02	$+0.20 \pm 0.05$
(n, n') [22]	+0.41	
(p, p') [29]	-0.34	+0.25
(p, p') [43]	-0.55	+0.33
(p, p') [23]	+0.41	
(d, d') [24]	+0.45	
(α, α') [25]	+0.36	
(α, α') [30]	$-0.32 \pm .01$	$+0.08\pm0.01$
(¹⁶ 0, ¹⁶ 0') [44]	-0.34	





G Kaur et al., Phy Rev C 97, 064606 (2018)



YK Gupta et al., Physics Letters B 845 138120 (2023)

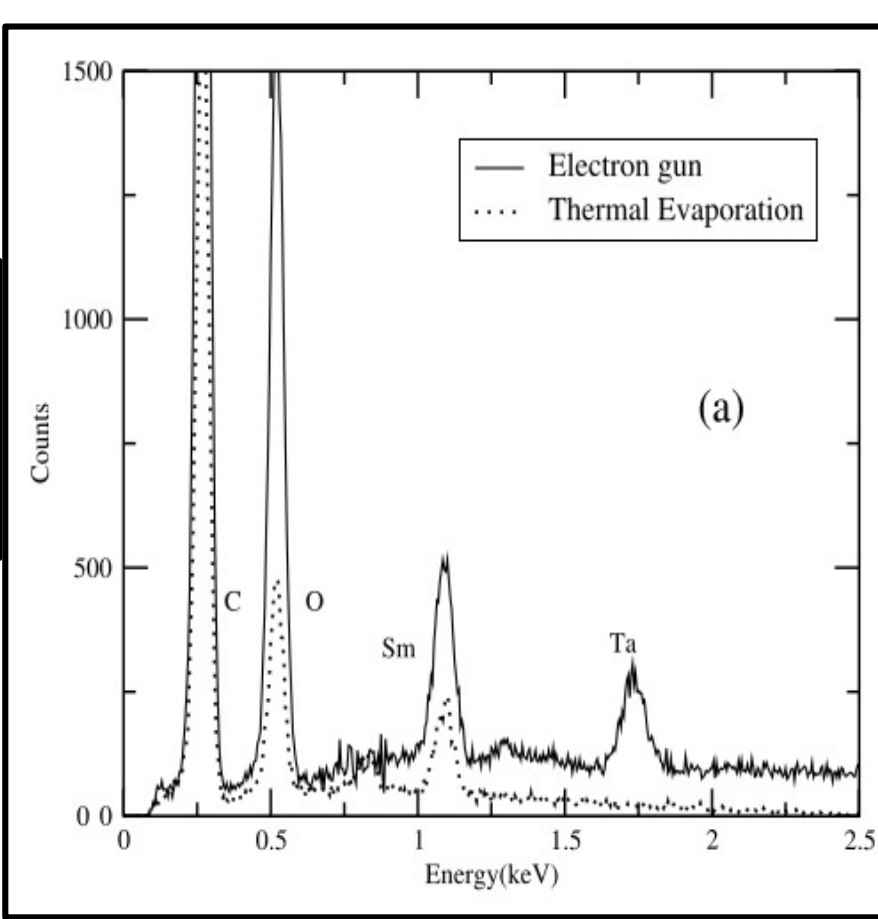
TARGET PREPARATION

^{144,154}Sm Target Preparation

- For QE measurements, the targets should be thin and self supporting to reduce the energy spread/lossf beam as well as of the reaction products in the target thickness..
- The self supporting targets for Sm isotopes is difficult to prepare because of highly oxidising nature.







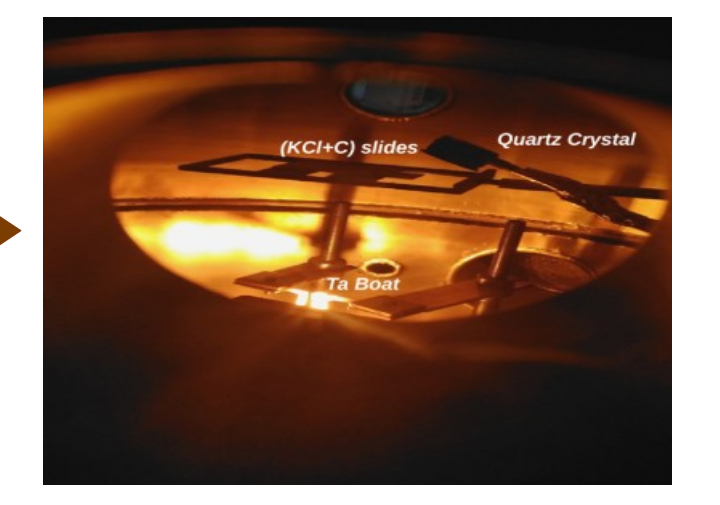
(a) High Vacuum evaporator at IUAC, New Delhi. (b) Inside View of the Chamber.

EDS spectrum (at 15 keV) of the samarium target prepared by Resistive Heating deposition and Electron gun deposition.

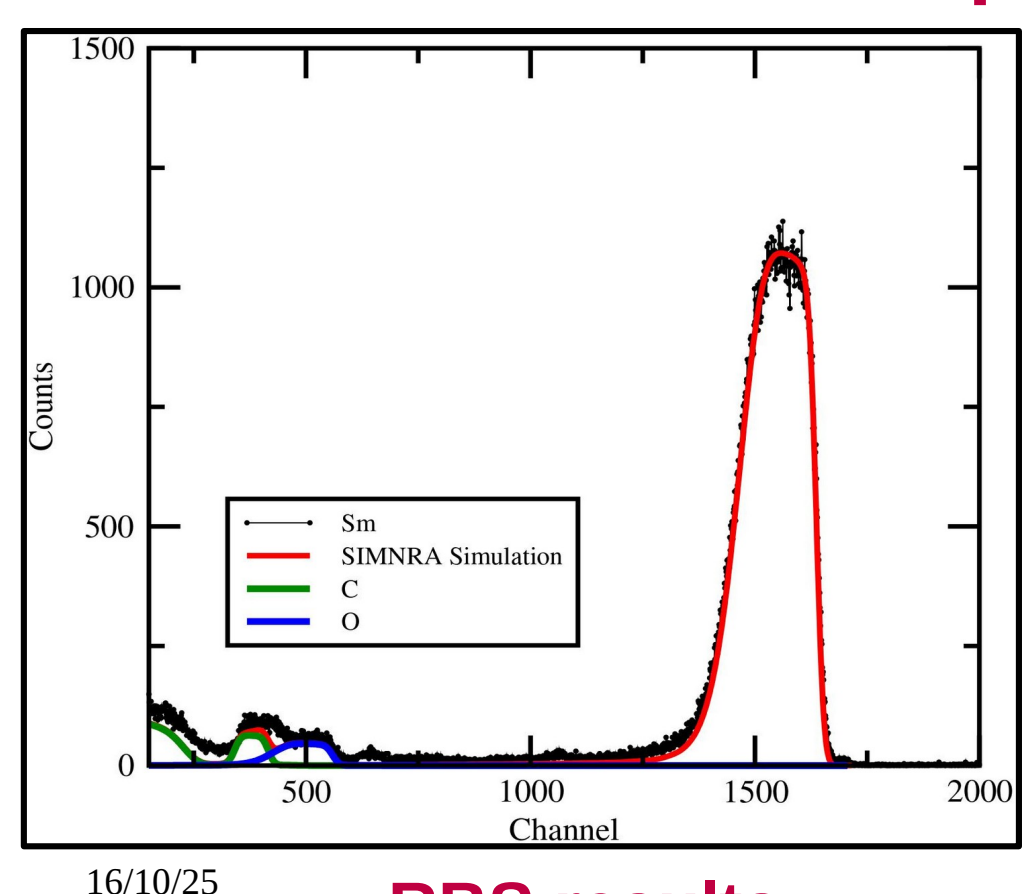
16/10/25

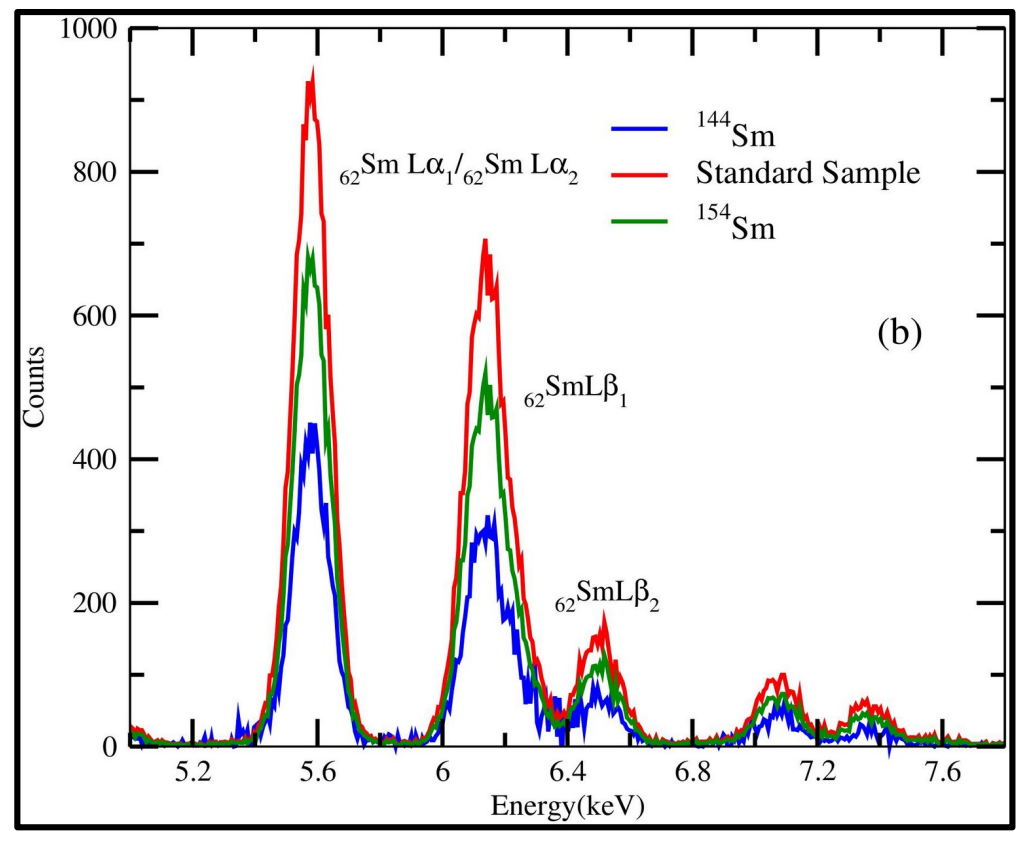
ISOTOPIC DEPOSITION with thermal evaporation

Inside View of the chamber during thermal evaporation



Characteristaion of prepared 144,154Sm Targets





RBS results

XRF results

19

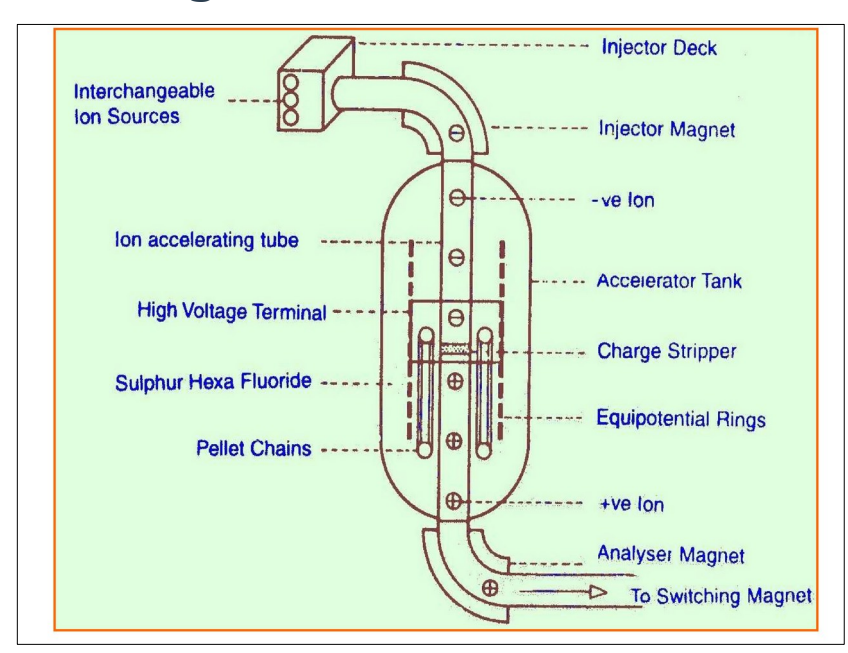
Experimental Facility



- For carrying out the experimental measurements, the experiments have been performed using the General Purpose scattering chamber (GPSC) of IUAC, New Delhi and the beam has been accelerated using the Pelletron accelerator shown in figure below.
- The energy in the Pelletron accelerator is calculated using the formula

$$E=E_i+(q+1)V_T$$

 Here, V_T is the terminal potential and q is the charge state used.



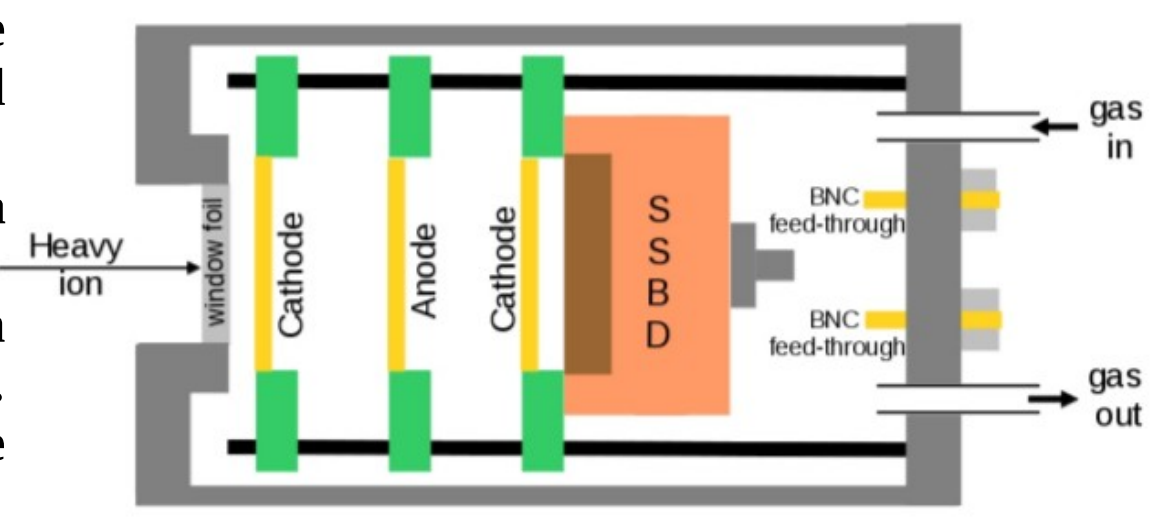
www.iuac.res.in/

Detection Facility: HYTAR

• HYTAR stands for HYbrid Telescope ARray. It is an array of the hybrid telescope developed at IUAC.

• It consists of a gas ΔE detector and a silicon stop E detector.

- The thickness of the ΔE detector can be varied by varying the gas pressure.
- Isobutane gas is used to operate the detectors at pressure 10-100 Torr.



Hybrid telescope detector

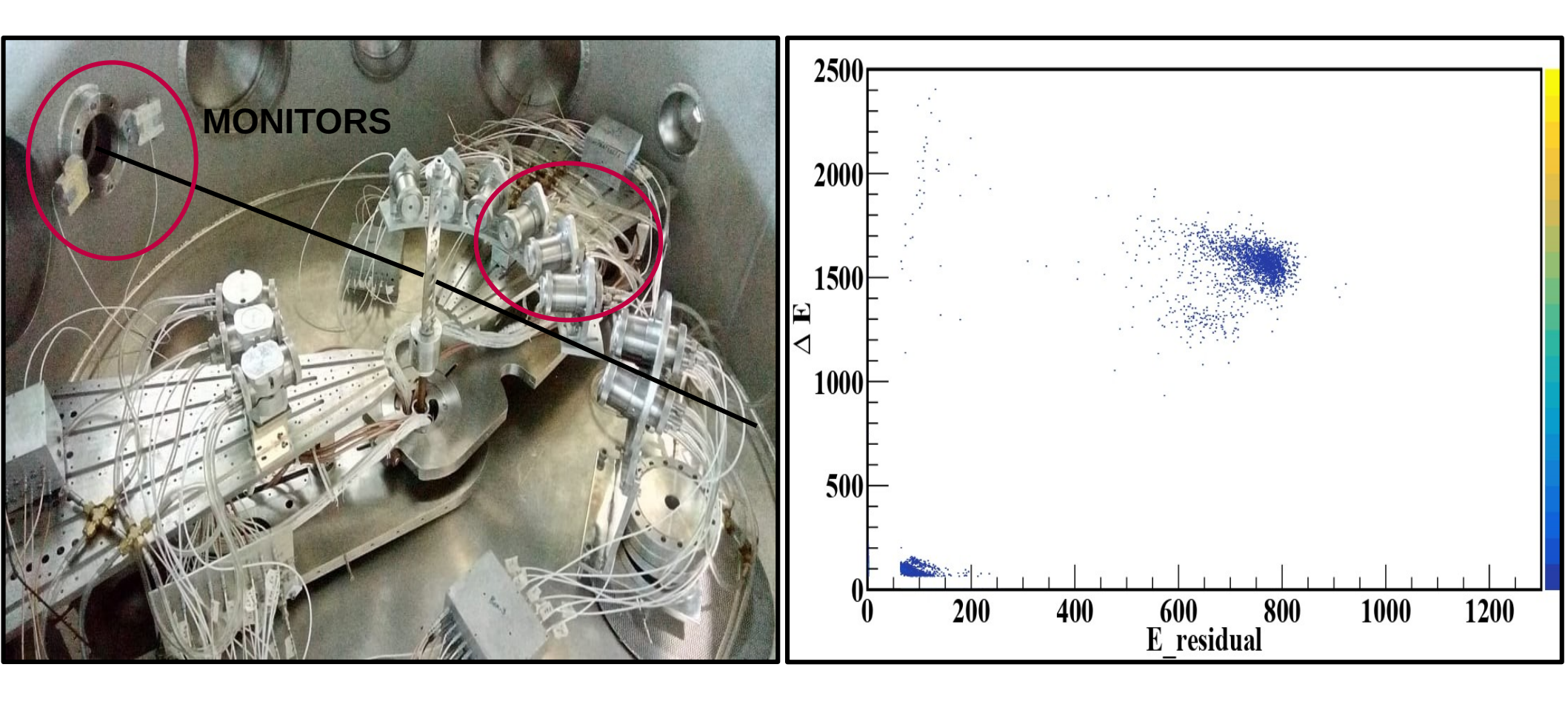
Advantages of HYTAR over Si $\Delta E-E$ detectors

For using Si as ΔE detector, the thickness of the detector should be around 10-40 μm . This thin Si detectors are prone to radiation damage and are also opaque to low energy heavy ions. By replacing the Solid state detector with the gas detector, the thickness can be varied as per the ions to be detected by just varying the gas pressure

A. Jhingan et.al. Nuclear Inst. and Methods in Physics Research, A 903 (2018) 326–334

Experiment SET-UP: QE-BD for 28Si+144Sm

- This experiment was performed in GPSC of IUAC using pelletron beam and HYTAR detection facility.
- Monitor detectors: SSBD
- Measurements: Quasi-elastic events
- Beams: ²⁸Si
- Target: 144 Sm ($\sim 103 \mu g/cm^2$)
 - Energy Range: (90-140)MeV for ²⁸Si
- Online Data Collection: FREEDOM



Pictorial View of the Set Up inside GPSC chamber and online spectra recorded.

Dome having 4 telescopes at 173°

EXPERIMENTAL ANALYSIS

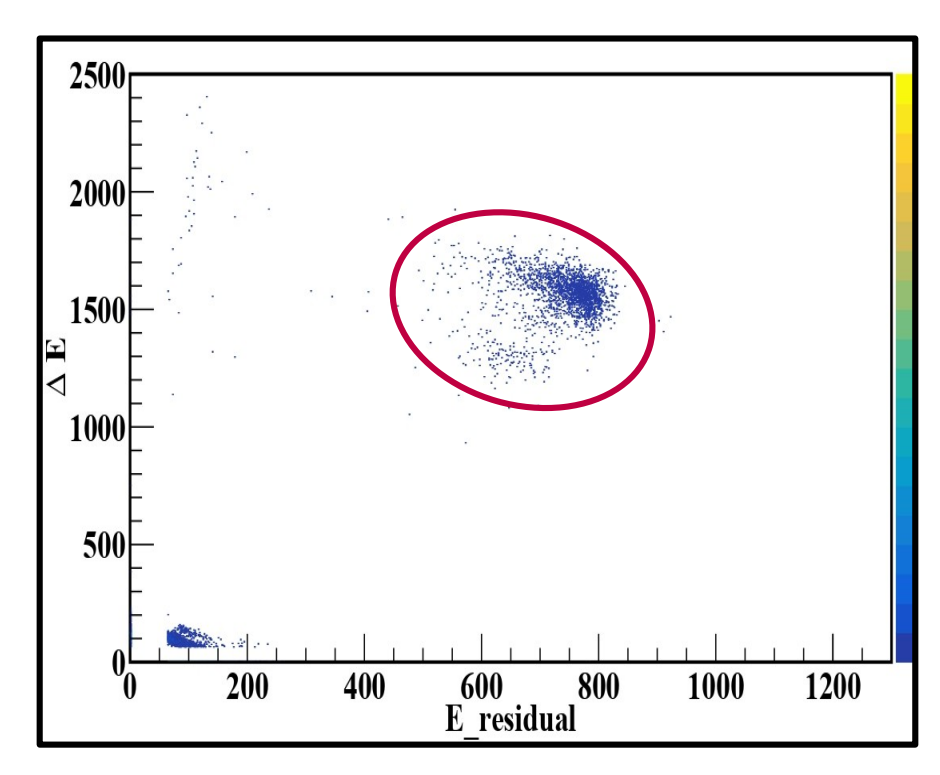
The quasi-elastic excitation function has been calculated

using formula

$$\frac{d\sigma_{qel}}{d\sigma_{Ruth}} = \frac{N_{tel}(E,\theta_{tel})}{N_{mon}(E,\theta_{mon})} \times \frac{\Delta\Omega_{mon}}{\Delta\Omega_{tel}} \times \frac{(d\sigma_{Ruth}/d\Omega)(E,\theta_{mon})}{(d\sigma_{Ruth}/d\Omega)(E,\theta_{tel})}$$

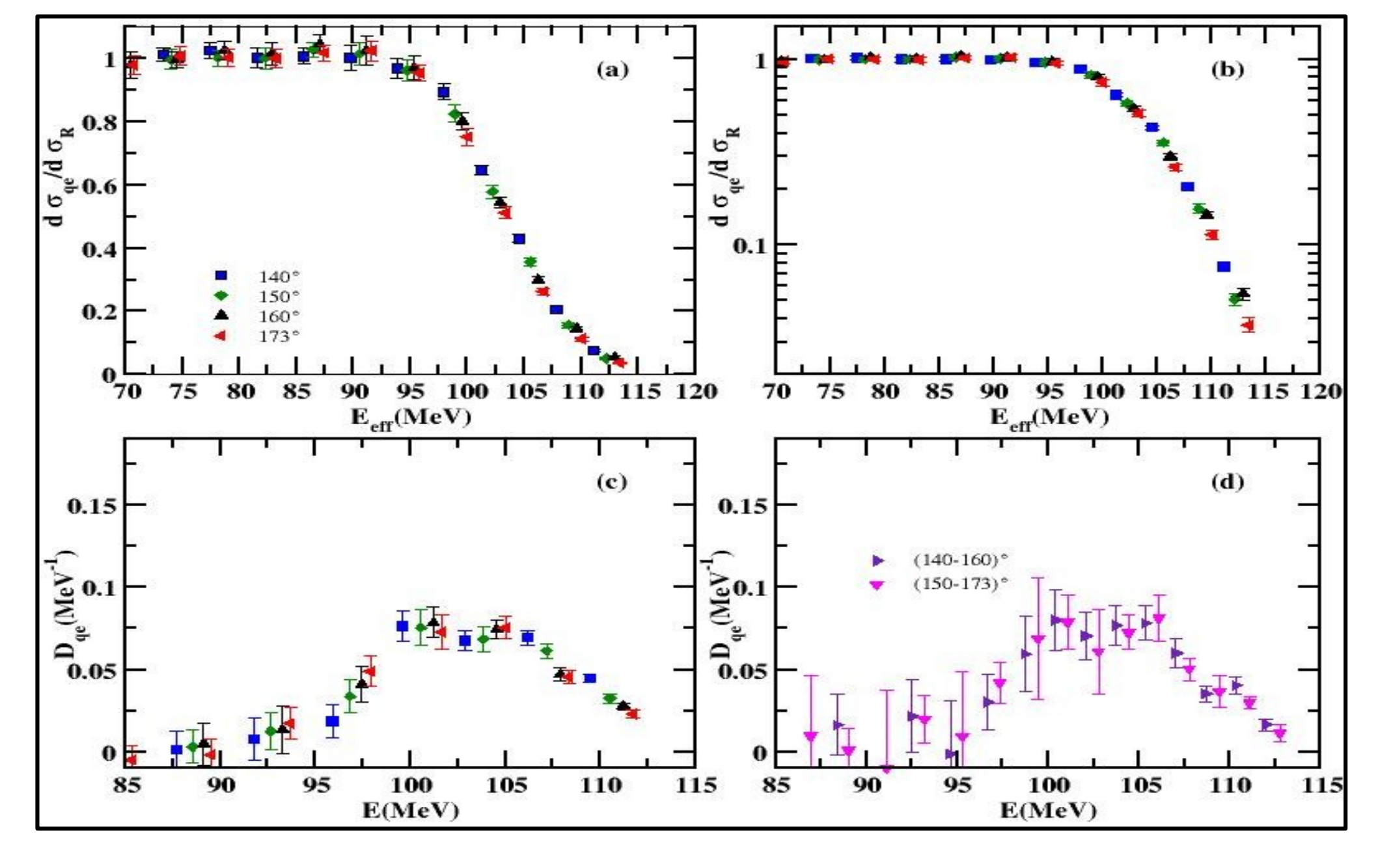
To extract the BD from the measured crosssection, the point difference formula has been employed

$$D_{qel}(E_{\text{eff}}) = -\frac{d}{dE_{\text{eff}}} \left[\frac{d\sigma_{\text{qel}}(E_{\text{eff}})}{d\sigma_{\text{R}}(E_{\text{eff}})} \right],$$



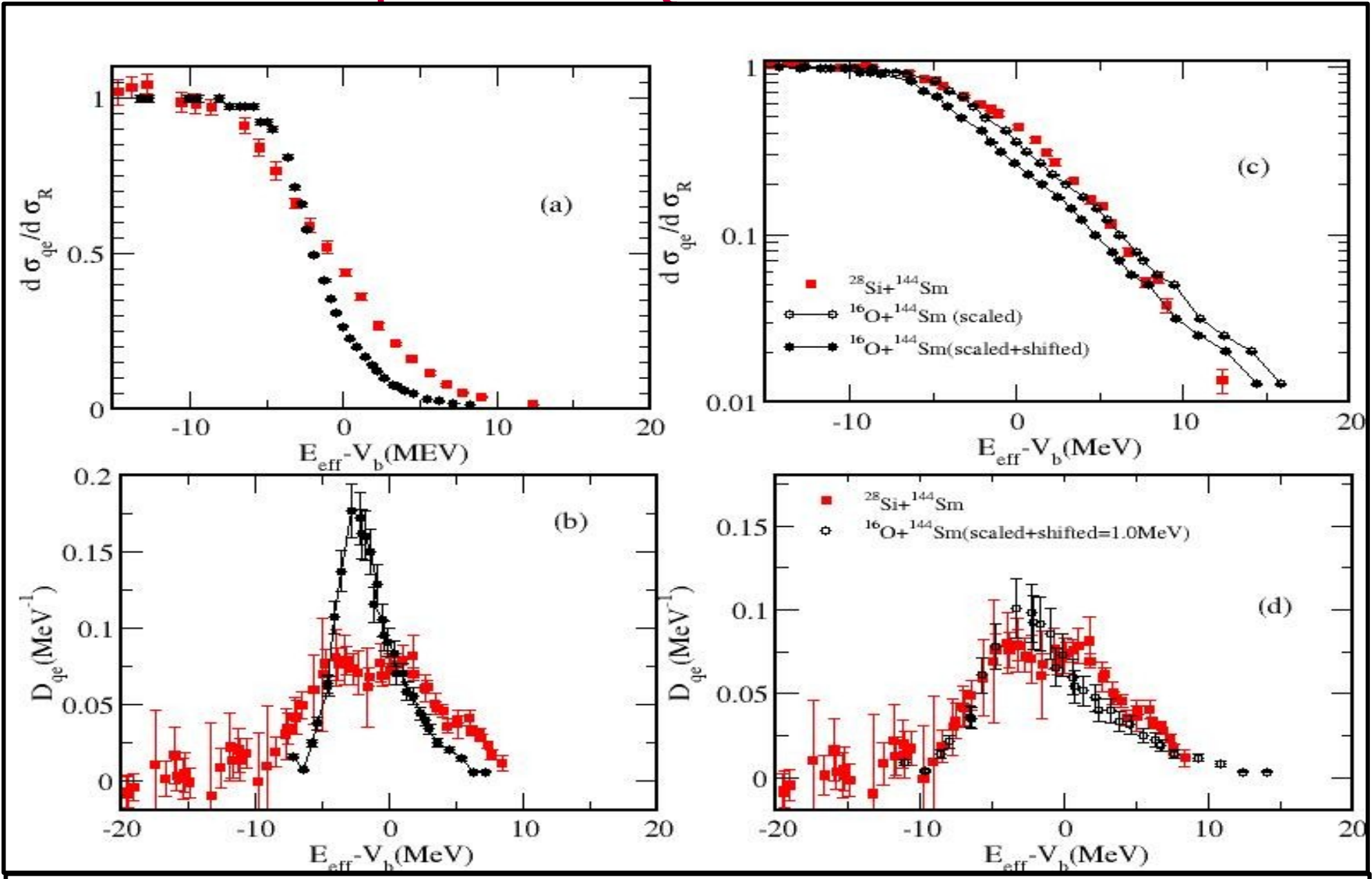
DISCUSSIONS:

²⁸Si + ¹⁴⁴Sm reaction



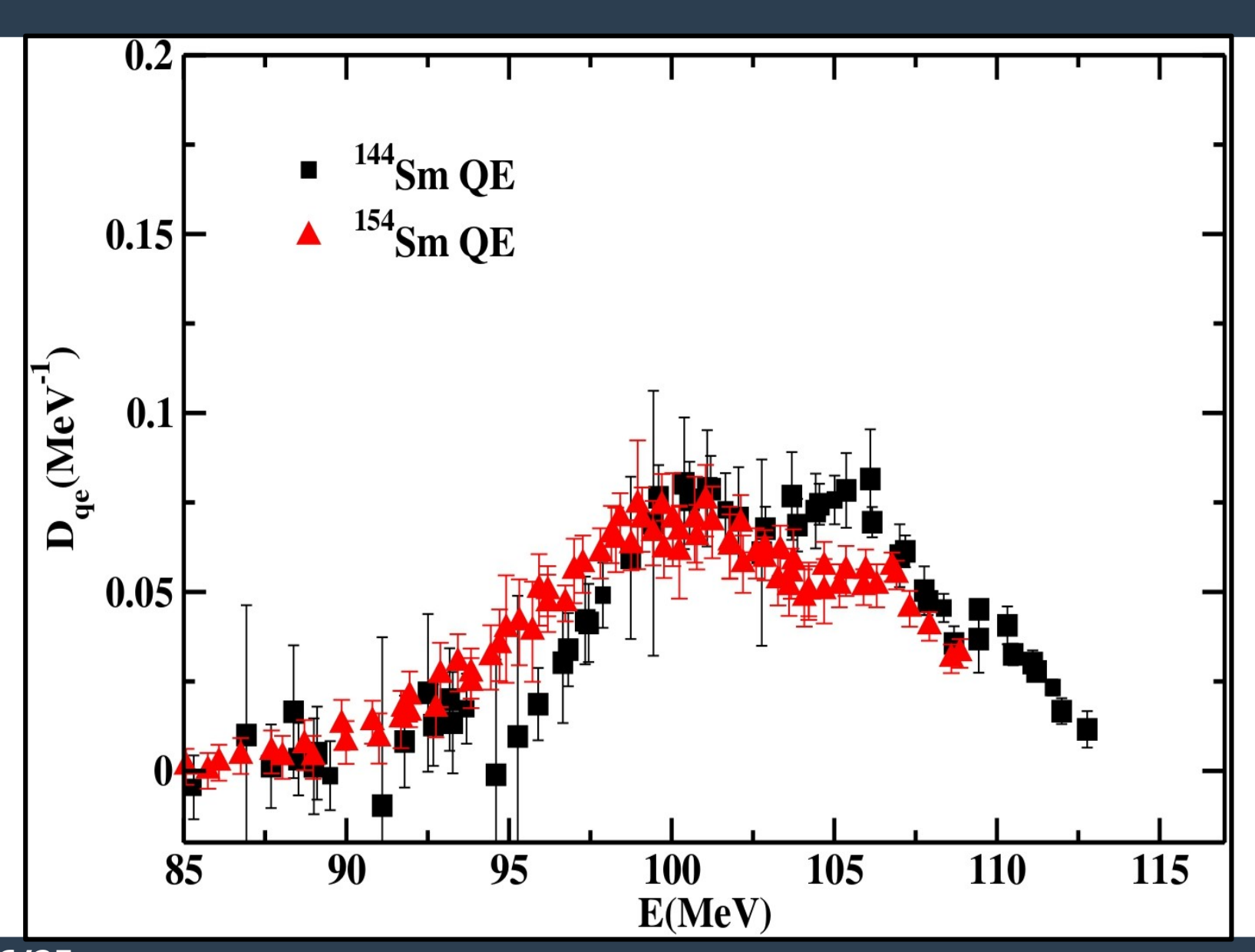
Quasielastic scattering excitation function plot for the 28 Si + 144 Sm system measured at four different angles (a) Linear Scale (b) Logarithmic Scale (c) Quasielastic BD plot extracted for the 28 Si + 144 Sm system measured at four different angles (d) using two angles data with Δ E=(1.8-2.2) MeV.

Comparison with QE-DATA of 16O+144Sm



Comparison between (a) QE-excitation function of ¹⁶O+ ¹⁴⁴Sm and ²⁸Si+ ¹⁴⁴Sm (b) BD of ¹⁶O+ ¹⁴⁴Sm and ²⁸Si+ ¹⁴⁴Sm (c) QE-excitation function of ¹⁶O+ ¹⁴⁴Sm (scaled+shifted) and ²⁸Si+ ¹⁴⁴Sm (d)BD of ¹⁶O+ ¹⁴⁴Sm (d)BD of ¹⁶O+ ¹⁴⁴Sm (scaled+shifted) and ²⁸Si+ ¹⁴⁴Sm (d)BD of ¹⁶O+ ¹⁴⁴Sm (scaled+shifted) and ²⁸Si+ ¹⁴⁴Sm (d)BD of ¹⁶O+ ¹⁴⁴Sm (scaled+shifted) and ²⁸Si+ ²

Comparison of BD of $^{28}\mathrm{Si}$ + $^{144}\mathrm{Sm}$ with $^{28}\mathrm{Si}$ + $^{154}\mathrm{Sm}$

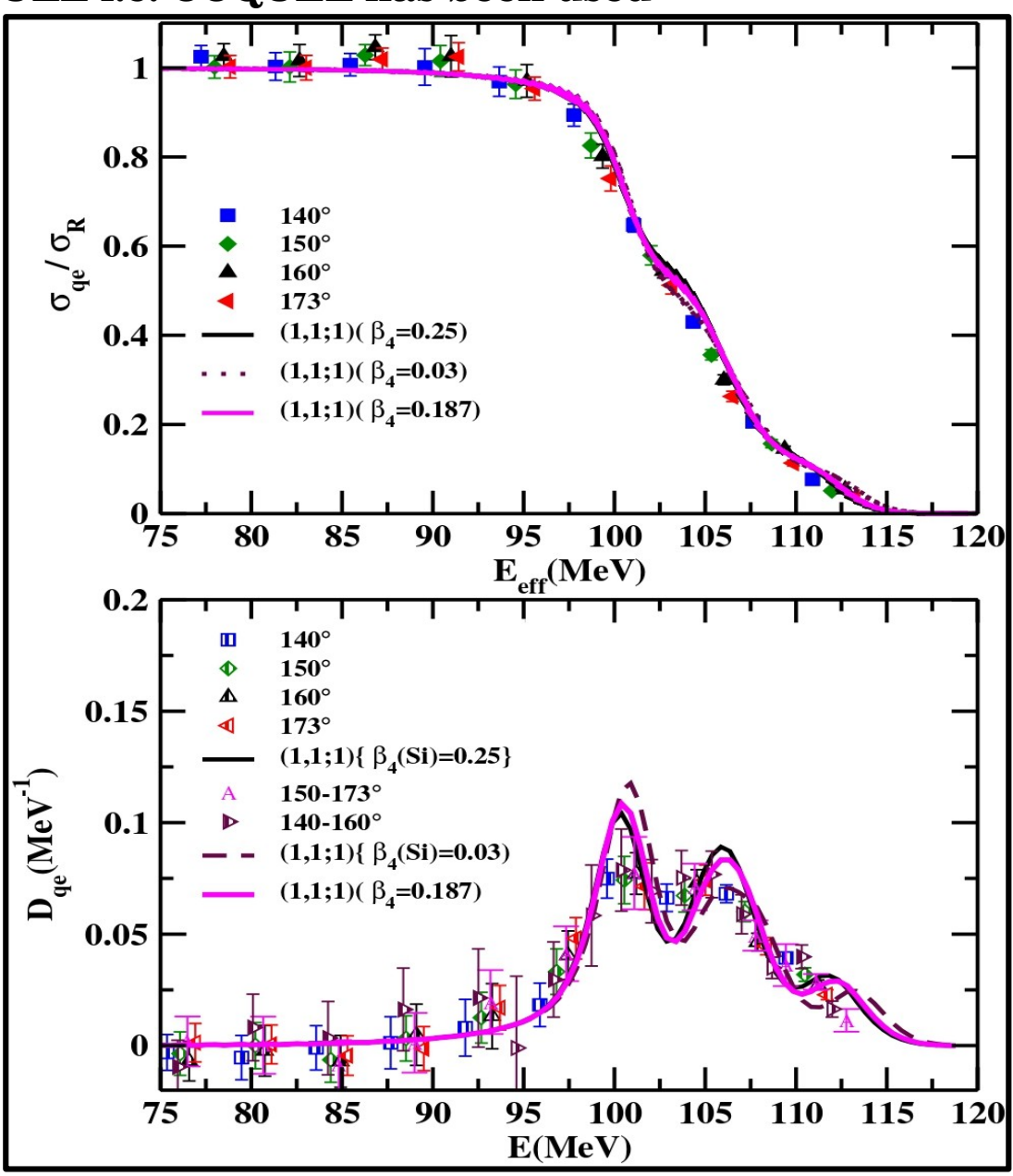


Coupled Channel Analysis For QE-Data

The scattering version of code CCFULL i.e. CCQUEL has been used

- The potential parameters used in the calculation corresponds to the Woods-Saxon potential parameters described as V_0 , r_0 and a_0 . The obtained value of parameters were $V_0 = 185$ MeV, $r_0 = 1.10$ fm and $a_0 = 0.72$ fm.
- The depth parameter value, radius parameter and the surface diffuseness parameter fixed during the calculation were 30 MeV, 1.0 fm and 0.3 fm.
- The calculations were performed including various types of couplings.

Nucleus	E _{exc}	Deformation parameter
²⁸ Si	E ₂₊ =1.77	$\beta_2 = -0.041$, $\beta_4 = 0.25$, $0.03, 0.18$
¹⁴⁴ Sm	E ₂₊ =1.66, E ₃₋ =1.81	$\beta_2 = 0.087, \beta_3 = 0.151$



Comparison between the experimental data and CC calculations under the different coupling schemes for the 28 Si + 144 Sm system.

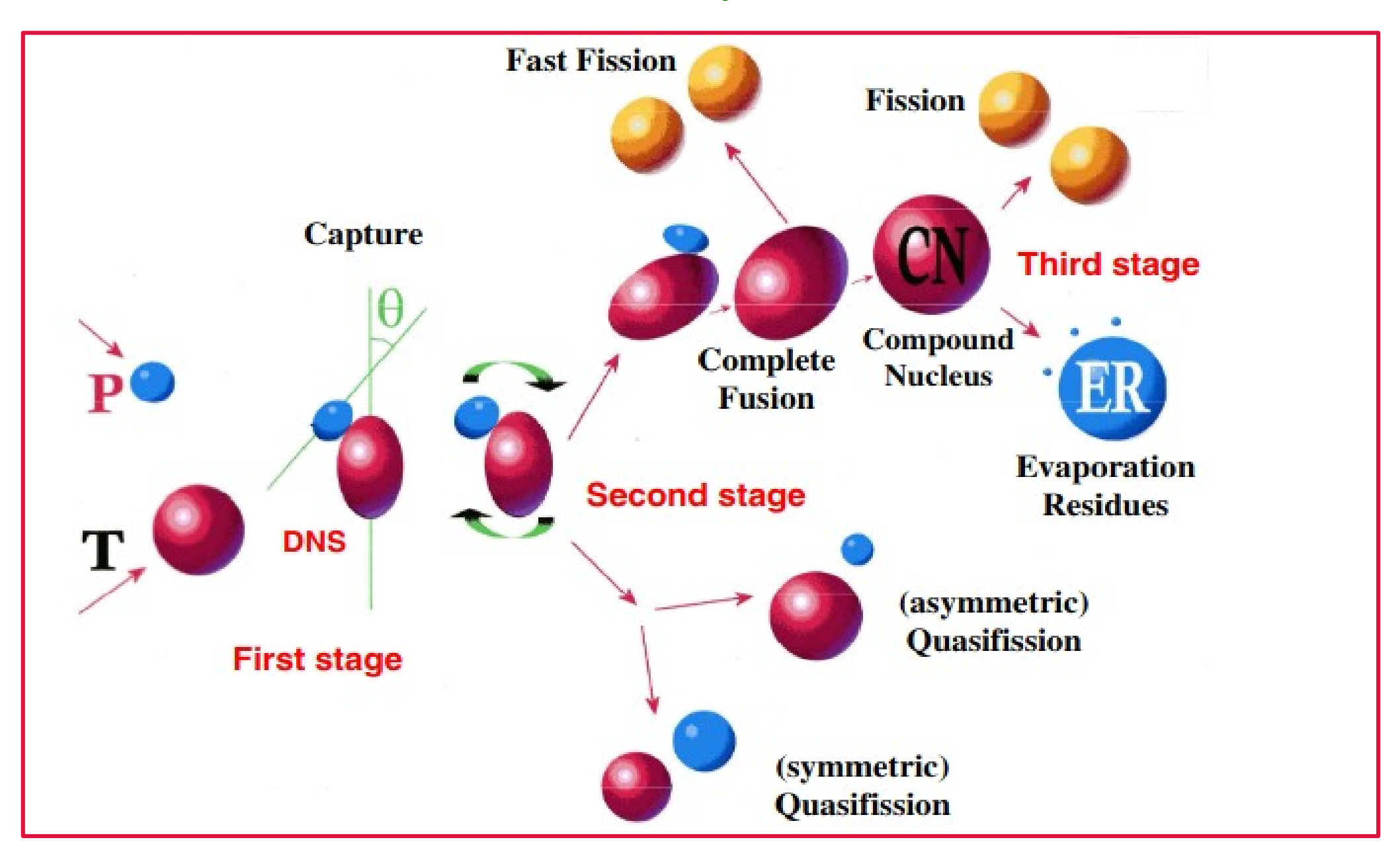
MAJOR CONCLUSIONS

- Distinct multiple peaklike structures were observed in the extracted barrier distribution. To locate the effect of the coupling in the experimentally observed BD, a comparison with the ¹⁶O+ ¹⁴⁴Sm QE-data shows that ²⁸Si excitations reflects as peaklike structures at higher energy.
- The Quasi-elastic (QE) excitation function and the barrier distribution (BD) method yield distinct deformation parameters, with noteworthy disparities in their outcomes.
- The QE-BD approach exhibits a notably higher positive hexadecupole value compared to the excitation function method, establishing a clear contrast in their predictions.
- This raises the question of employing QE as a potential tool to extract nuclear deformation parameters, while not taking dissipation effects into consideration

(Manuscript prepared)



Reaction Dynamics



MASS DISTRIBUTION STUDY: EXPERIMENTAL SET-UP & MOTIVATION

This experiment was performed in GPSC of VECC using beam from K130 Cyclotron.

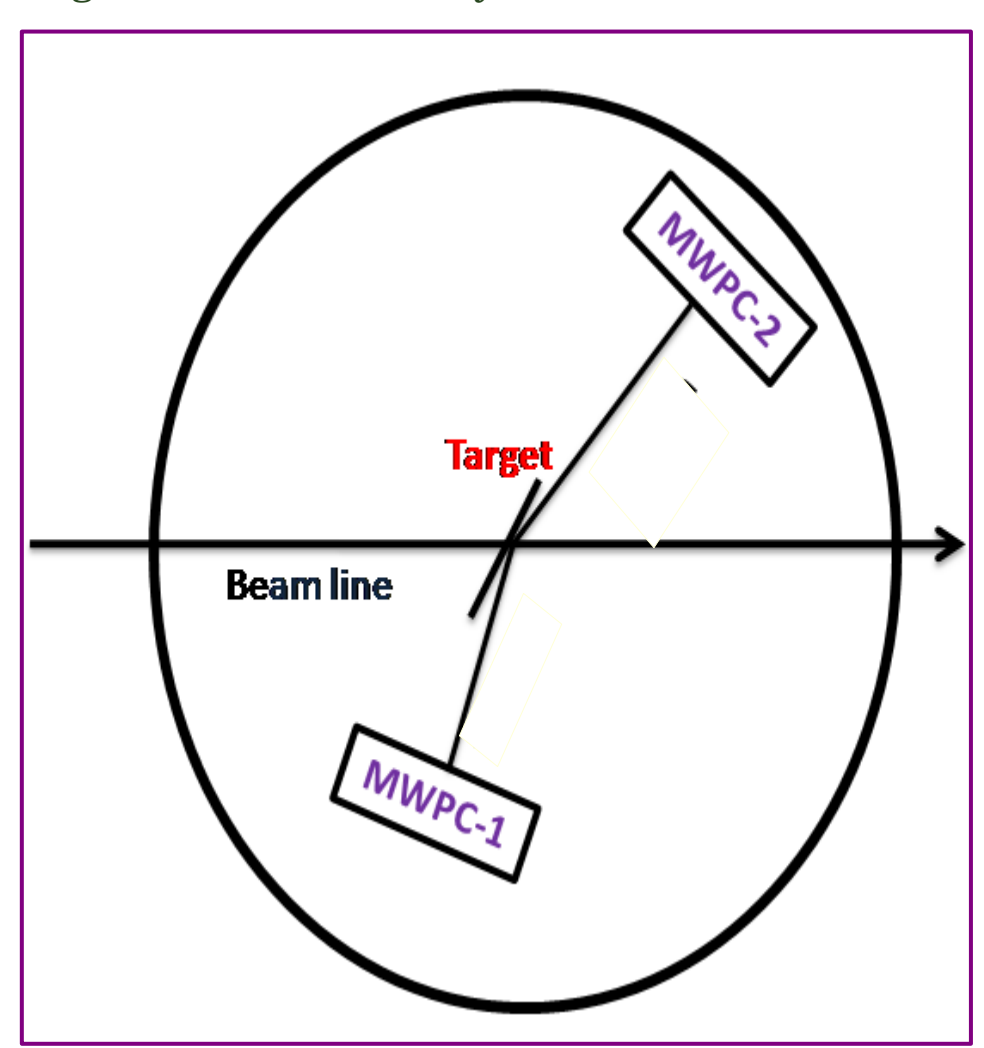
Beam: ¹⁶O

Beam energy 116-160 MeV

Target: 181Ta, 197Au, 205Tl, 208Pb

MOTIVATION:

- The excitation energy dependence of the fission fragment mass and folding angle distributions for heavy ion induced reactions on preactinides targets well above the Coulomb barrier energies are not well known due to the scarcity of data.
- The purpose is to understand the fusion fission dynamics well above the Coulomb barrier energies; particularly to address if the theoretical models that are valid near the Coulomb barrier can explain the fission data at high energies.



DETECTION FACILITY

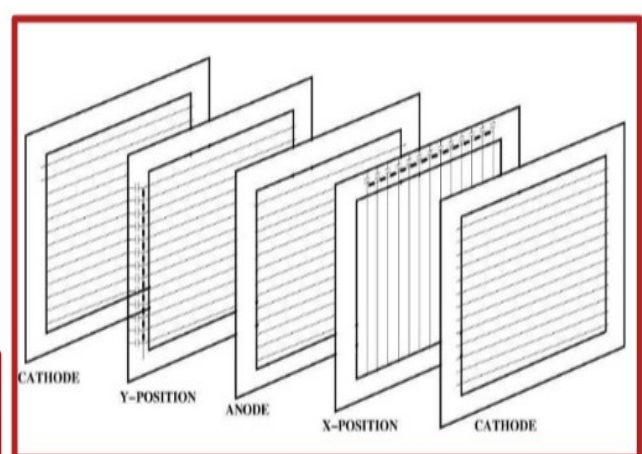
Employed the in-house developed Multi Wire Proportional Counters to record the interested events



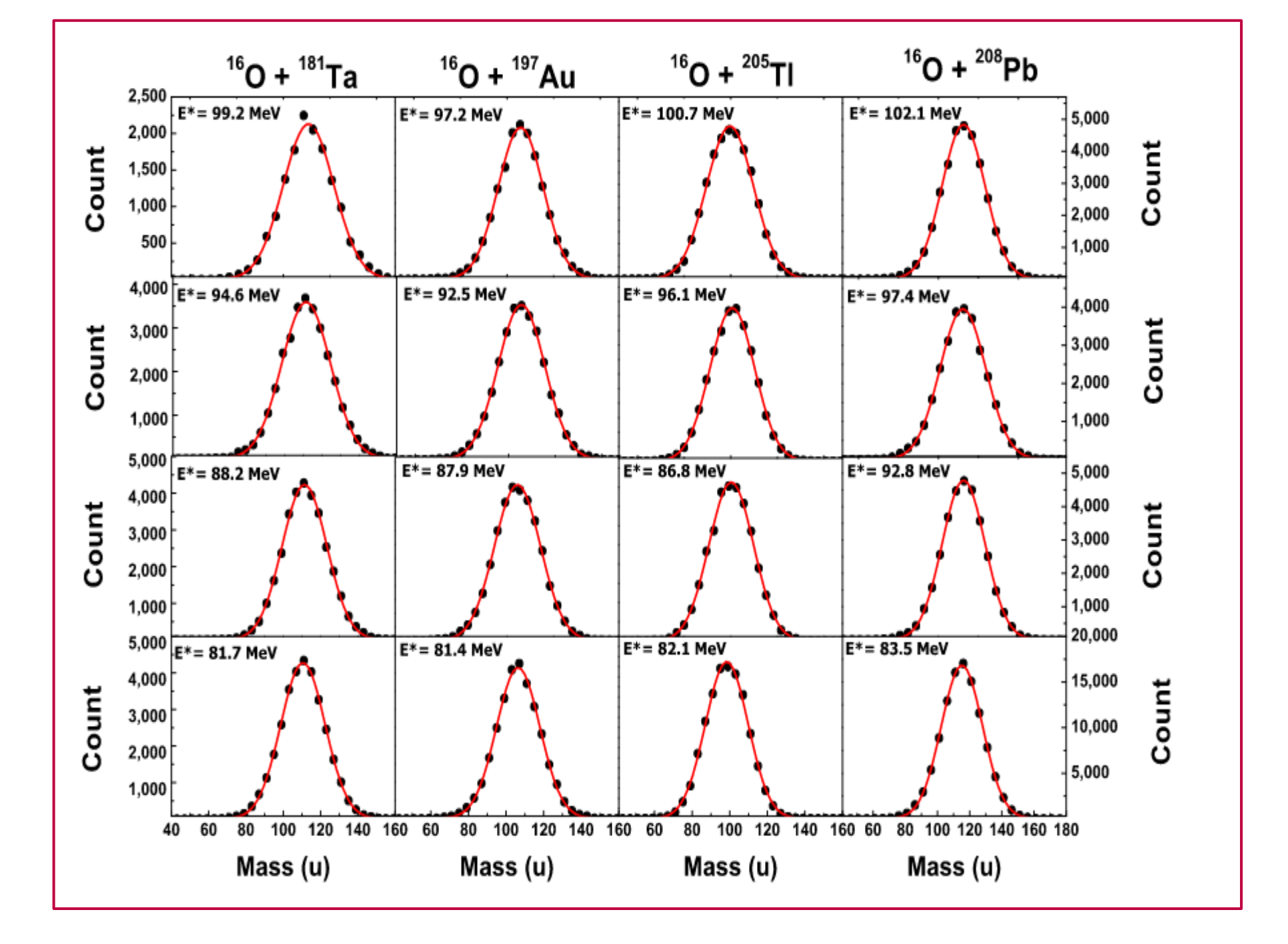




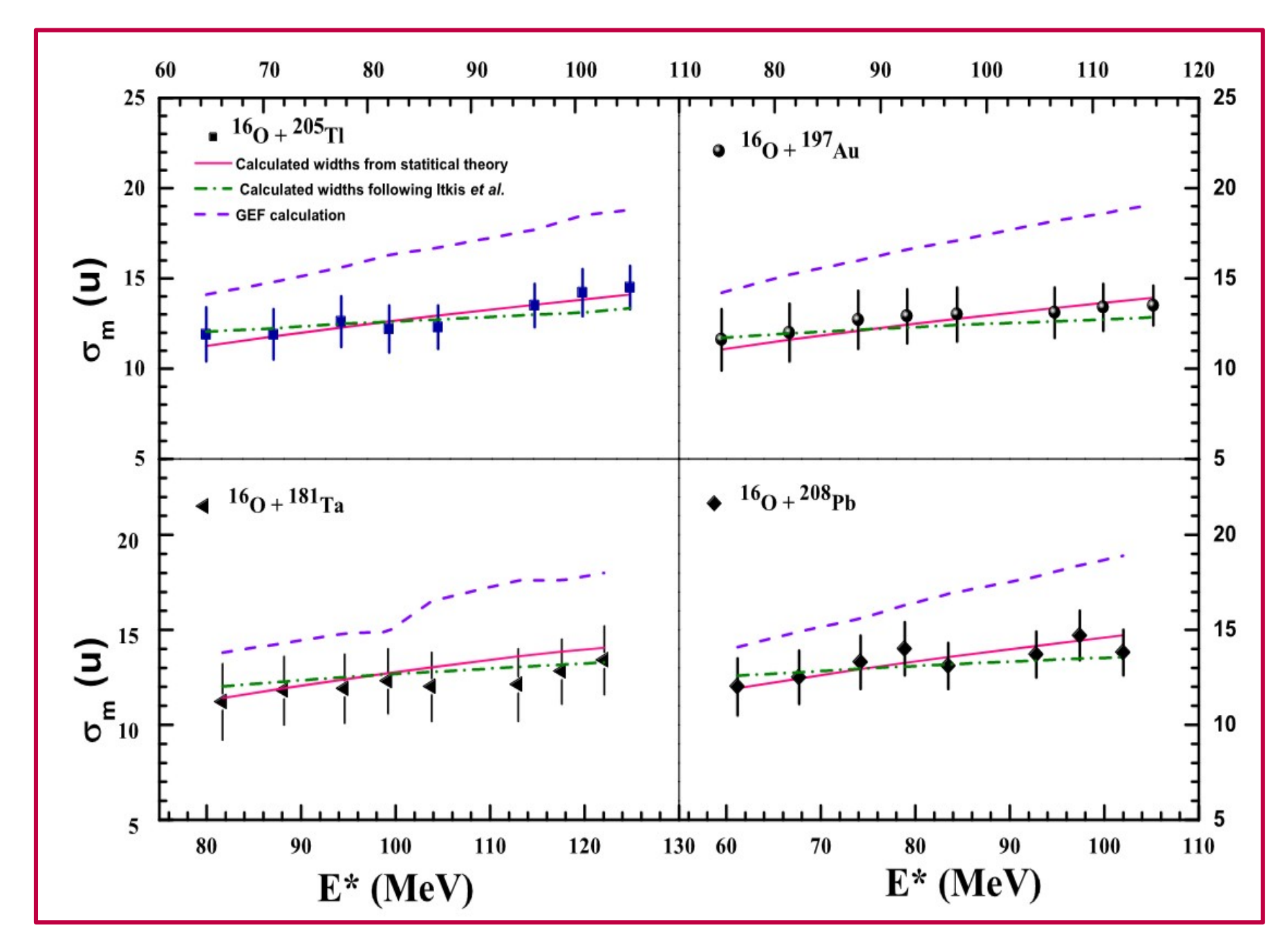
Assembled MWPC



Inside wire plate arrangement

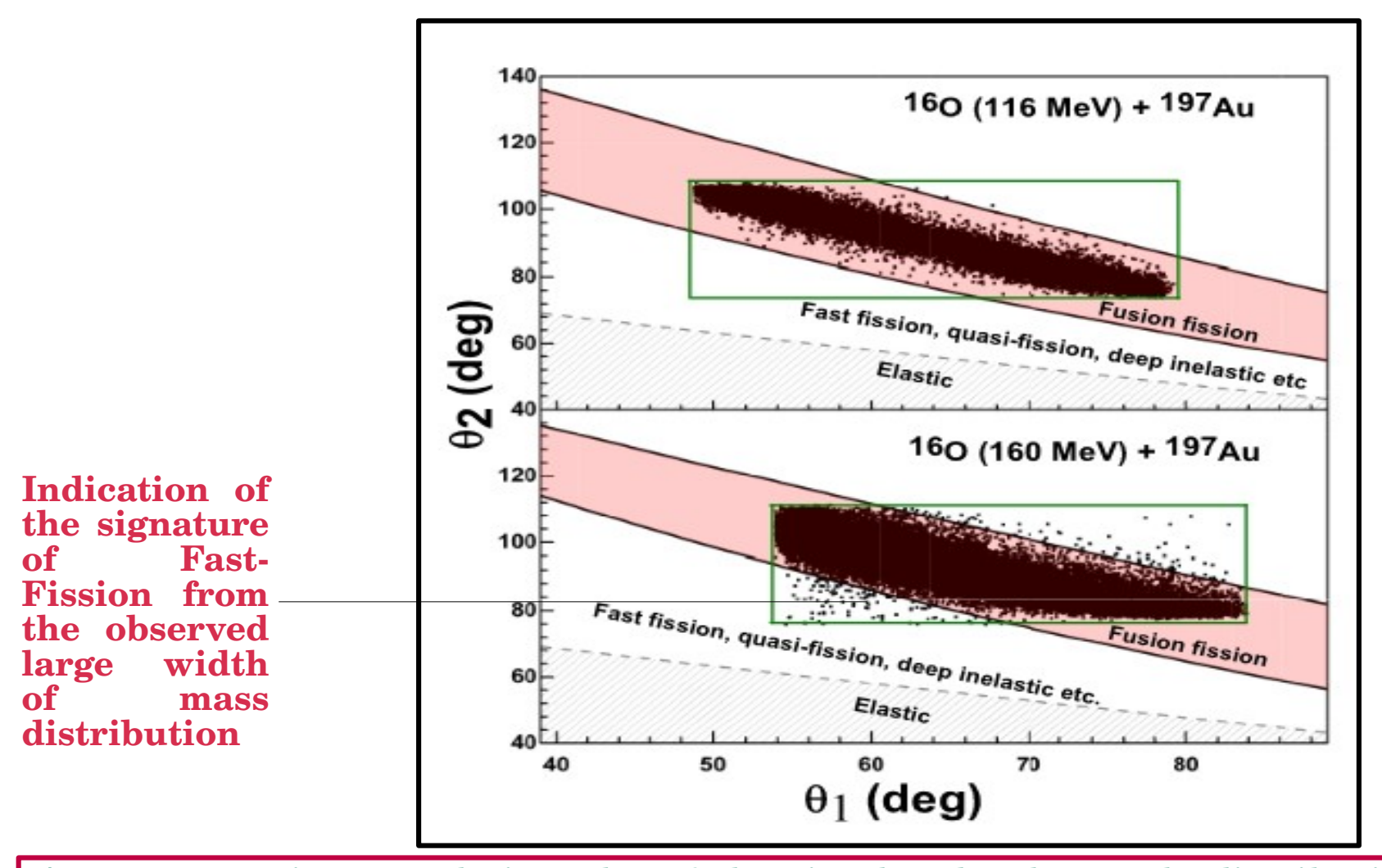


The mass distributions of complementary fission fragments for the reactions $^{16}O + ^{181}Ta$, $^{16}O + ^{197}Au$, $^{16}O + ^{205}Tl$ and $^{16}O + ^{208}Pb$ at the mentioned excitation energy.



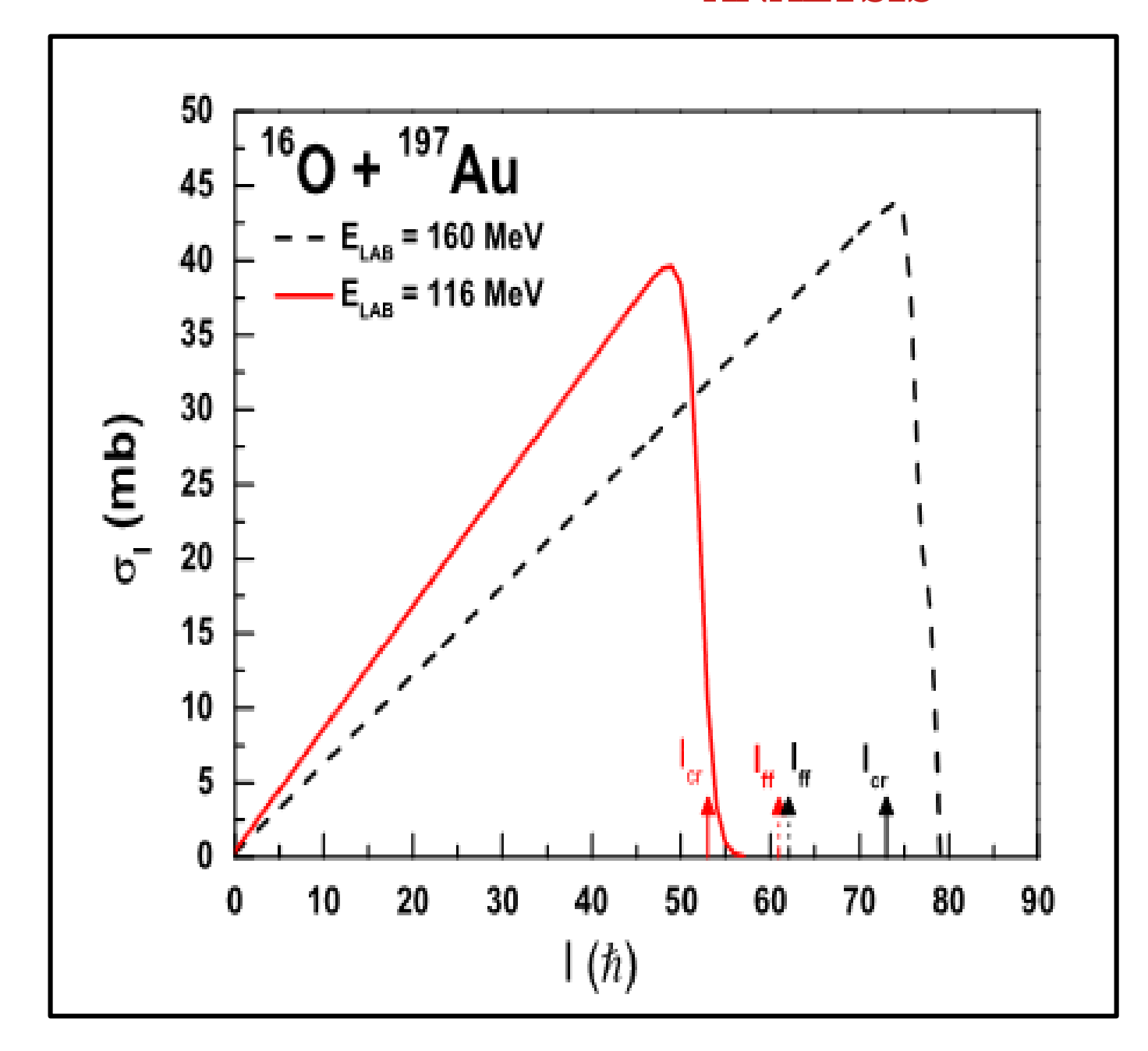
Variation of the measured standard deviation $\sigma_m(u)$ of the mass distributions with excitation energy.

RESULTS OF K130 EXPERIMENT



A representative correlation plot of the simulated polar angle distributions of the events produced in the reaction ^{16}O + ^{197}Au at the lowest (above) (116 MeV) and highest (below) beam energy (160 MeV) measured in the experiment.

ANALYSIS



Adjacent figure shows the partial capture cross-sections as a function of angular momentum for ¹⁶O + ¹⁹⁷Au at projectile energies of 116 MeV and 160 MeV calculated with the coupled channels code CCFULL.

The values of $l_{\text{(Tsad>Bf=0)}}$ = 0 are obtained using the formulism given by A.J. Sierk, PRC 33, 2039 (1986).

RESULTS AND SUMMARY

- Reaction mechanism for ¹⁶O + ¹⁸¹Ta, ¹⁶O + ¹⁹⁷Au, ¹⁶O + ²⁰⁵Tl and ¹⁶O + ²⁰⁸Pb have been studied in the above experiment and fission fragment folding angle distributions and mass distributions for all the systems were predominantly symmetric Gaussian, which indicates the fusion fission dynamics is dominant at well above Coulomb energies.
- The results show that fissioning nucleus distributions are consistent with statistical model predictions for reactions well above the Coulomb barrier energies.
- Half mass asymmetry calculation shows a contribution of the fast-fission collisions in the tail part of the mass distribution.

PHYSICAL REVIEW C 109, 064620 (2024)

Neutron Multiplicity Measurements for α + 232 Th reaction

INTRODUCTION AND MOTIVATION: Fission neutron

multiplicity measurement in ²³⁶U

Scientific Motivation:

To understand the evolution of a compound nucleus (CN) in a path to fission

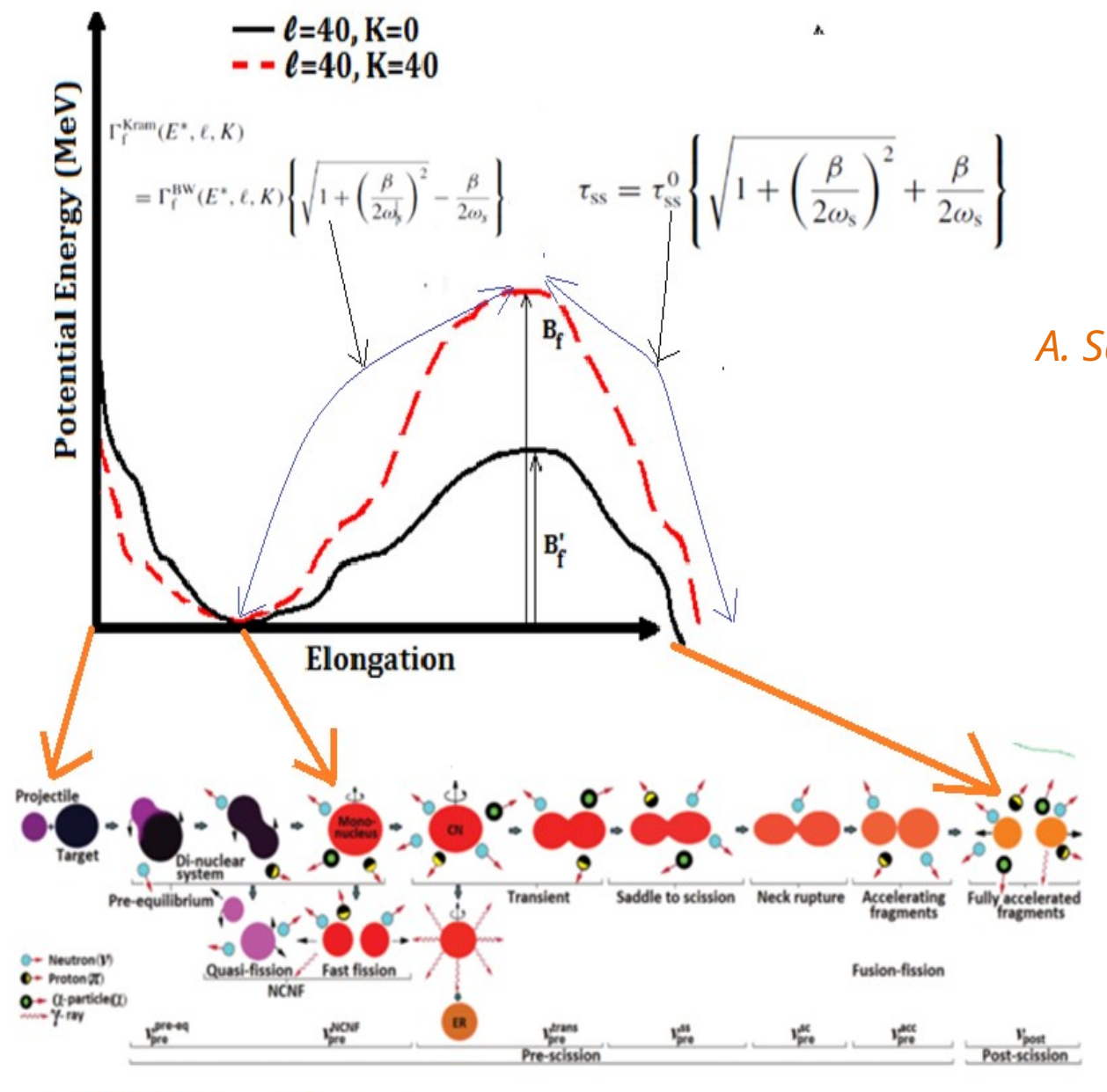
i) The pre-scission neutron multiplicity is one of the useful probe. (D. Hilscher et. al; Ann. Phys. 17, 471 (1992).)

The pre-scission neutron multiplicity (υ_{pre}): Number of neutron emitted per fission during the evolution of CN from its initial shape to scission point.

J. P. Lestone et. al; PRC 79, 044611 (2009).

Pre-scission neutron multiplicity is sensitive to dissipative dynamics occurs during the the evolution of a compound nucleus (CN) in a path to fission.

The evolution of a compound nucleus (CN) in a path to fission



A. Saxena et. al; PRC 49, 2 (1994)

Reduction in fission width using dissipative dynamics is proposed by Kramers.

$$\Gamma_{\rm f}^{\rm BW}(E^*,\ell,K=0)$$

$$= \frac{1}{2\pi \rho_{\rm g}(E^*)} \int_0^{E^* - B_{\rm f}(\ell)} \rho_{\rm s}(E^* - B_{\rm f}(\ell) - \epsilon) d\epsilon$$

 β is the dissipative coefficient.

Scientific Motivation ...

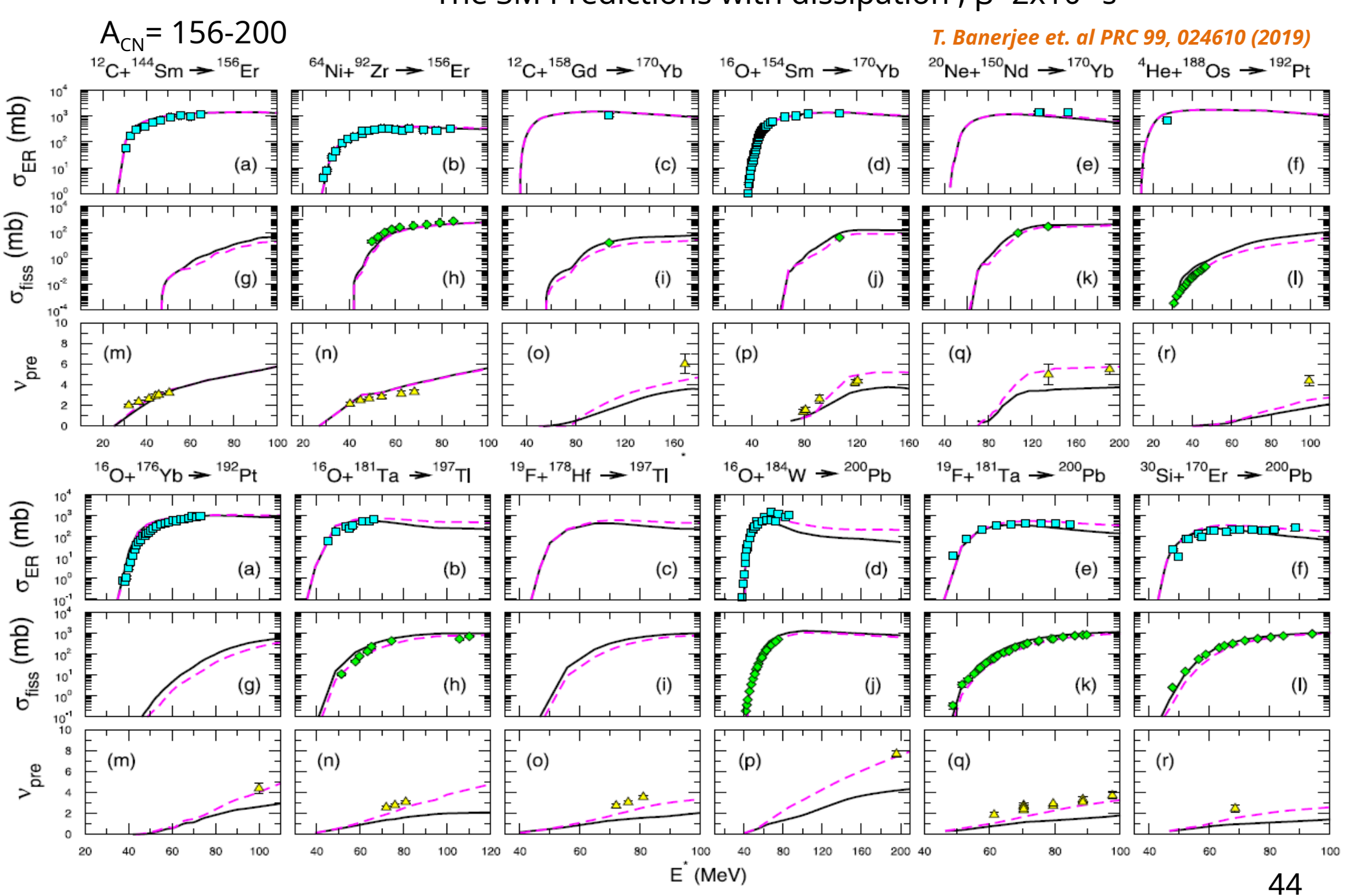
1. In a recent work, the statistical model simultaneously reproduce the measured $\sigma_{fission}$ & σ_{ER} but it failed to reproduce the υ_{pre} simultaneously with the other two for 158 < Δ_{CN} < 225.

2. Most of the earlier measurements are with heavy ions beam where contribution to the \mathbf{v}_{pre} from non compound processes like quasi-fission and fast-fission are present in data.

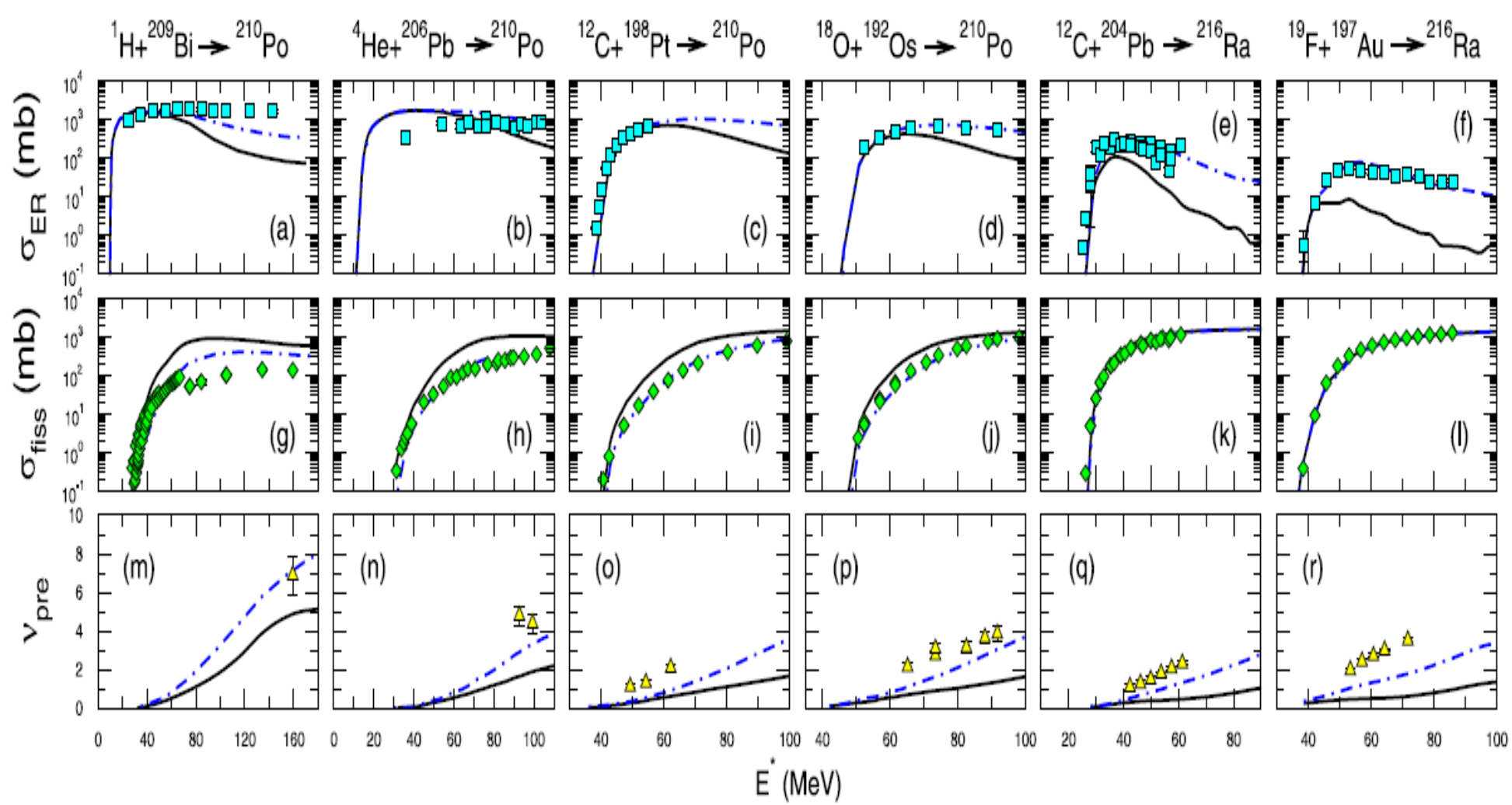
T. Banerjee et. al PRC 99, 024610 (2019)

The SM Predictions without any dissipation

-The SM Predictions with dissipation , $β=2x10^{21}s^{-1}$



 A_{CN} =210-216



T. Banerjee et. al PRC 99, 024610 (2019)

Scientific Motivation ...

- 1. In a recent work, the statistical model simultaneously reproduce the measured $\sigma_{fission}$ & σ_{ER} but it failed to reproduce the \mathbf{U}_{pre} simultaneously with the other two for 158 < \mathbf{A}_{CN} < 225.
- 2. Most of the earlier measurements are with heavy ions beam where contribution to the \mathbf{v}_{pre} from non compound processes like quasi-fission and fast-fission are present in data.

T. Banerjee et. al PRC 99, 024610 (2019)

Therefore we proposed fission neutron measurement using light ion beam for the $A_{\text{CN}} > 225$

System: ⁴He +²³²Th---²³⁶U

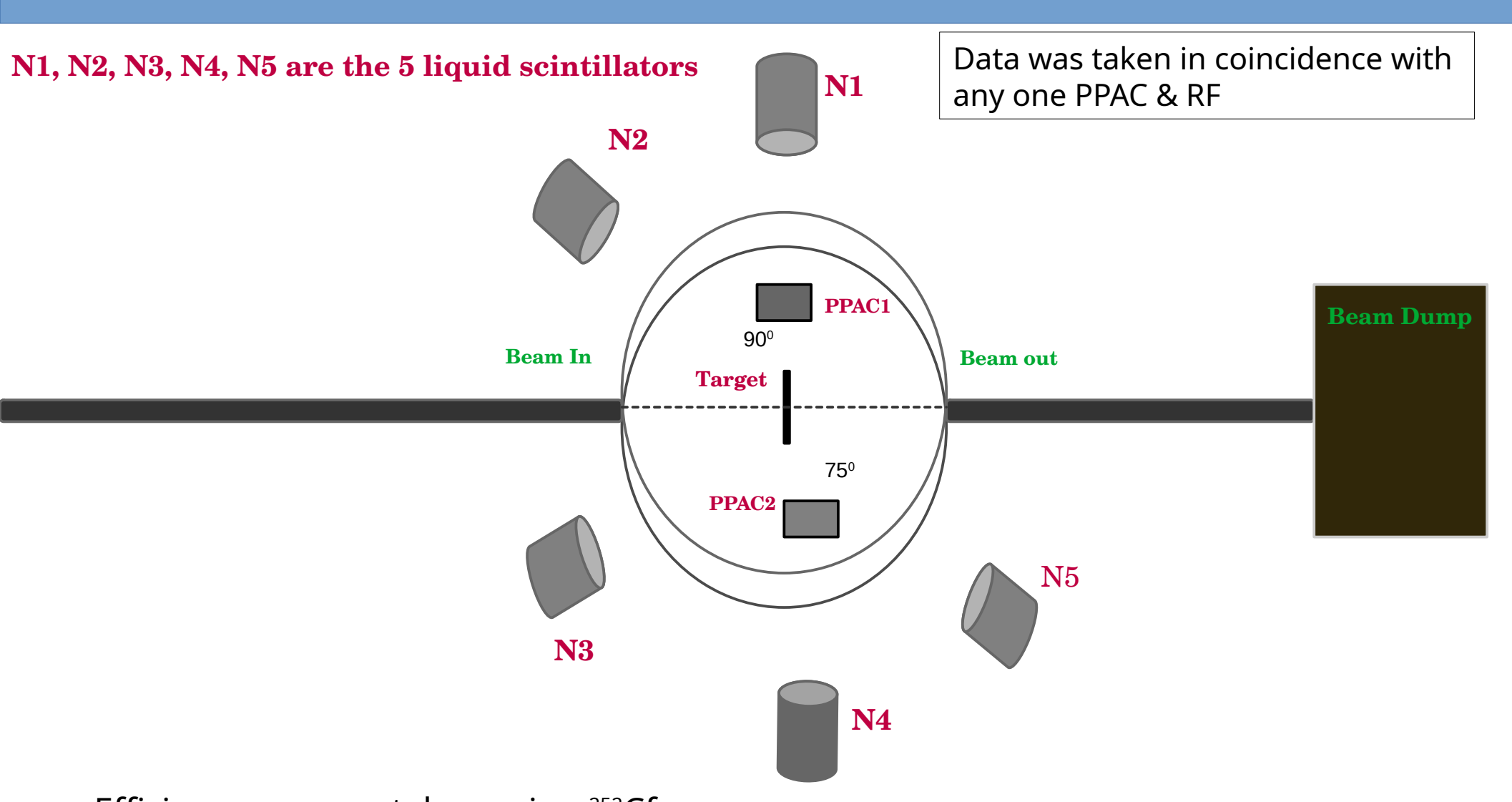
From present work, we will try to estimate the dissipation strength β for a range of CN as for this system, it is expected to be pure compound nuclear fission & **extracted** β **value will give true dispassion strength.**

Experimental Details

- An experiment was conducted using K130 RTC beam.
- Detectors: 2 PPAC inside the scattering chamber for recording the fission events and 5 liquid scintillator (BC501A) detectors were set up outside the scattering chamber, 1.25 meters from the target center
- Beam: ⁴He
- Target: ²³²Th (~2.3 mg/cm²)
- Energy Points: 26 MeV, 29 MeV, 34 MeV, 40 MeV, 44 MeV
- Online Data Collection : VME based data acquisition system

E _{lab} (MeV)	E*(CN)(MeV)
26	20.98
29	23.93
34	28.85
40	34.74
44	38.68

Experimental Set Up



Efficiency run was taken using ²⁵²Cf source

Details of detection methods

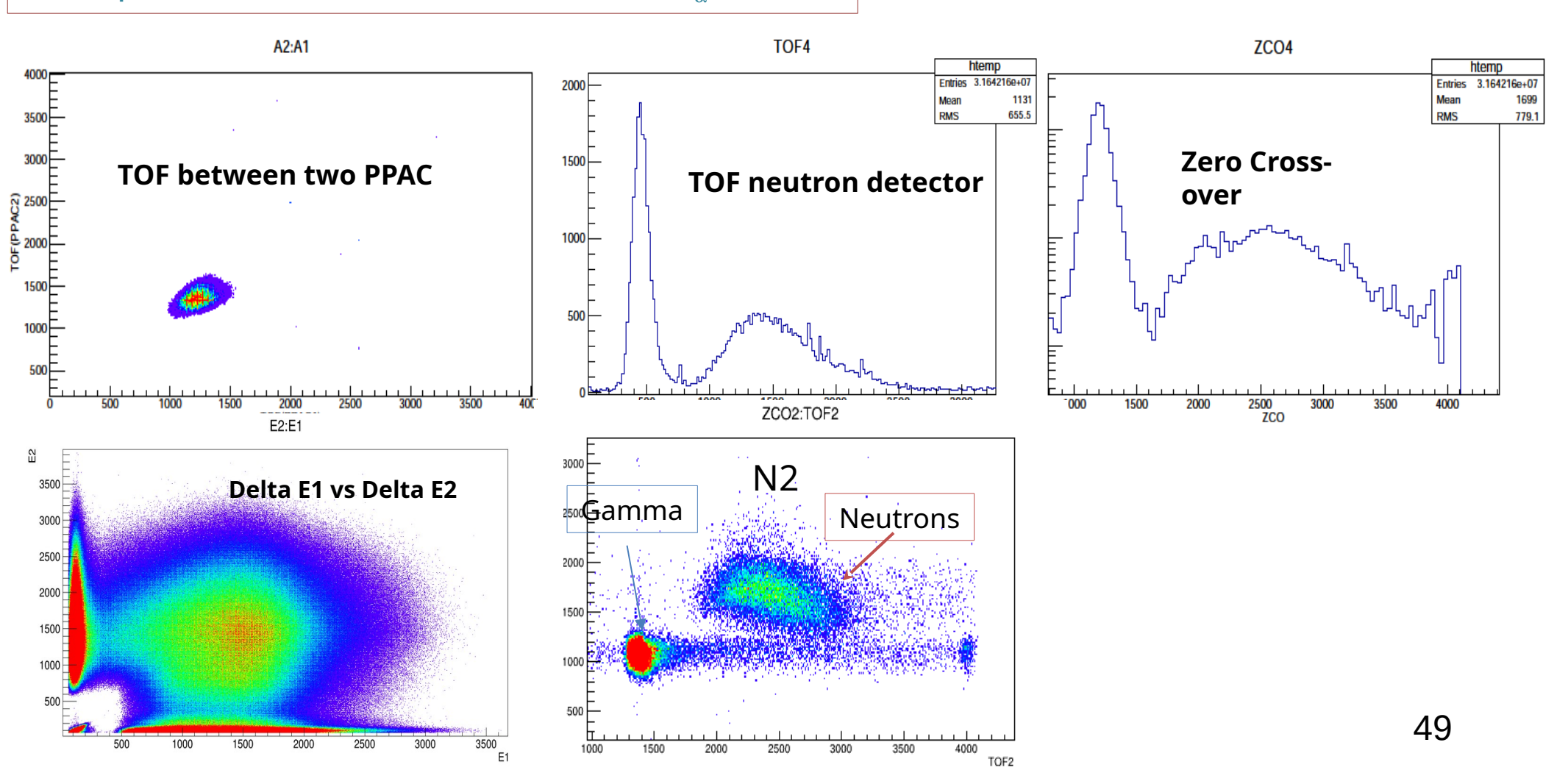
Fission fragments were detected in Parallel Plate Avalanche Counters(PPAC)

- i) Mass----Time of flight (TOF) technique with respect to the RF signal of VECC cyclotron.
- ii) Energy loss----From the amplitude of PPAC signals

Neutron were detected in liquid scintillator detectors

i) **Energy**---- Time of flight (TOF) technique with respect to the RF signal.

Raw spectrum for ${}^{4}\text{He} + {}^{232}\text{Th}$ reaction at $E_{\alpha} = 29$ MeV



DATA ANALYSIS

The main aim of this analysis is to extract pre- and post-scission components

of neutron multiplicity. The data analysis part comprises the following steps:

- A) Neutron detection efficiency
- B) Conversion of TOF spectra to neutron energy spectra
- C) Extraction of neutron multiplicity

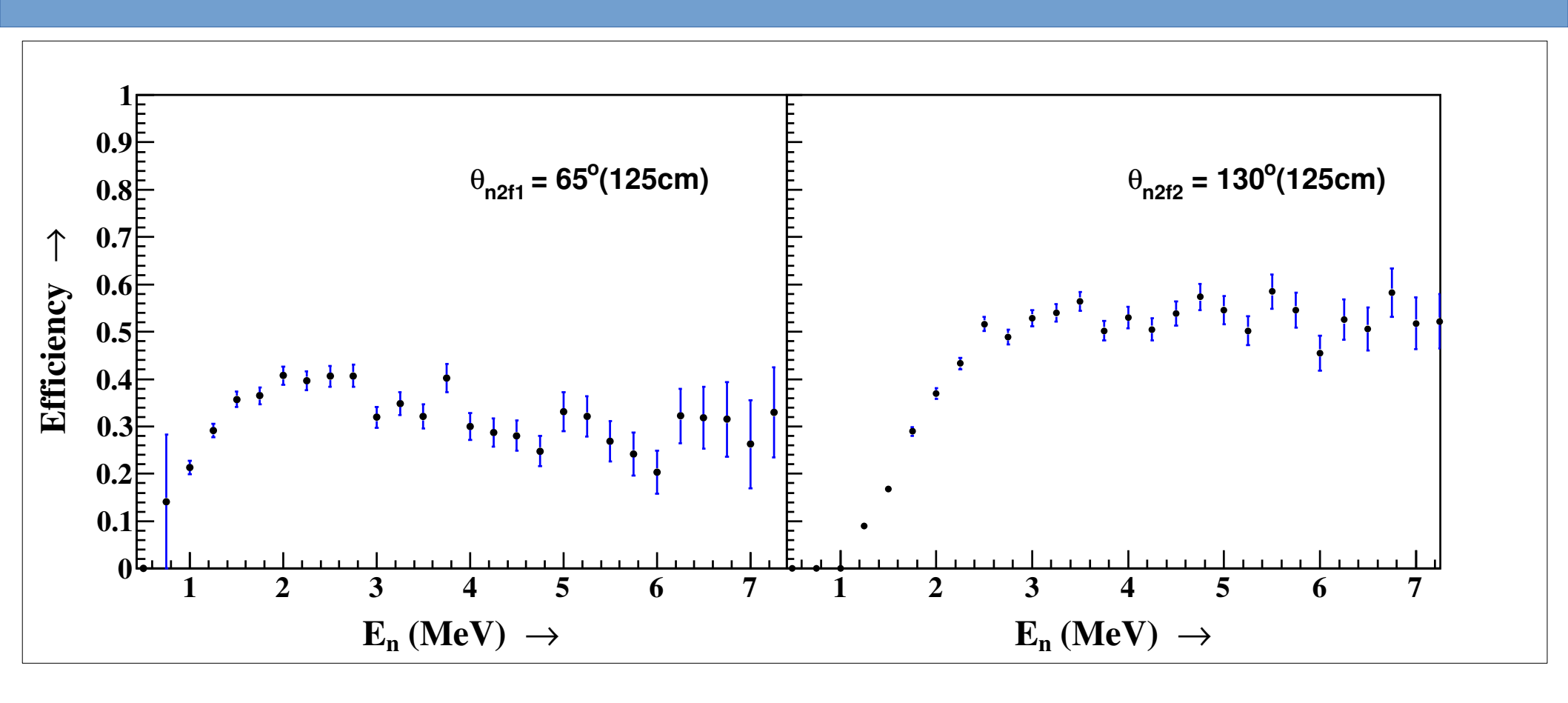
EFFICIENCY OF NEUTRON DETECTORS

- The primary task is to analyse the efficiency of the neutron detectors used.
- The efficiency of each detector was analysed experimentally by measuring the neutron energy spectrum using $^{252}{\rm Cf}$ source.
- For the TOF spectrum, the start signal was provided by the timing signal of the PPAC and the stop signal was generated from the neutron detector. The neutron energy deduced from the calibrated TOF was gated with the PPAC timing and the energy loss signal to efficiently select events from fission only and also with the neutron lobe as shown in previous slide 49.
- Standard ²⁵² Cf source energy spectrum was normalised with neutron multiplicity ν = 3.77, the neutron detector solid angle and total number of fission detected.
- The Maxwellian neutron energy spectrum of the ²⁵²Cf is given as

$$ref = rac{2\sqrt{E}_{lab}exp(rac{-E_{lab}}{T})}{\sqrt(\pi)T^{rac{3}{2}}}$$

The intrinsic efficiency of the neutron detector was determined by taking ratio of the experimentally measured energy to the Maxwellian predicted energy spectrum.

Efficiency Plot (Preliminary) of one of the detector N2



Neutron detector efficiencies can vary with the choice of reference fragment or timing counter—contrary to previous studies.

Neutron Energy Spectra

- TOF spectra were calibrated using a precision TAC calibrator and the prompt γ -ray peak as reference.
- To distinguish the neutrons from γ rays, a two-dimensional neutron gate (TOF vs ZCO)
 and the energy loss signal from PPAC and 1D gate of PPAC position was applied over the
 calibrated TOF spectra.
- The calibrated and gated TOF spectra were converted into the neutron energy (E_n)
 spectra.
- The neutron energy spectra were further corrected with the above obtained efficiency.

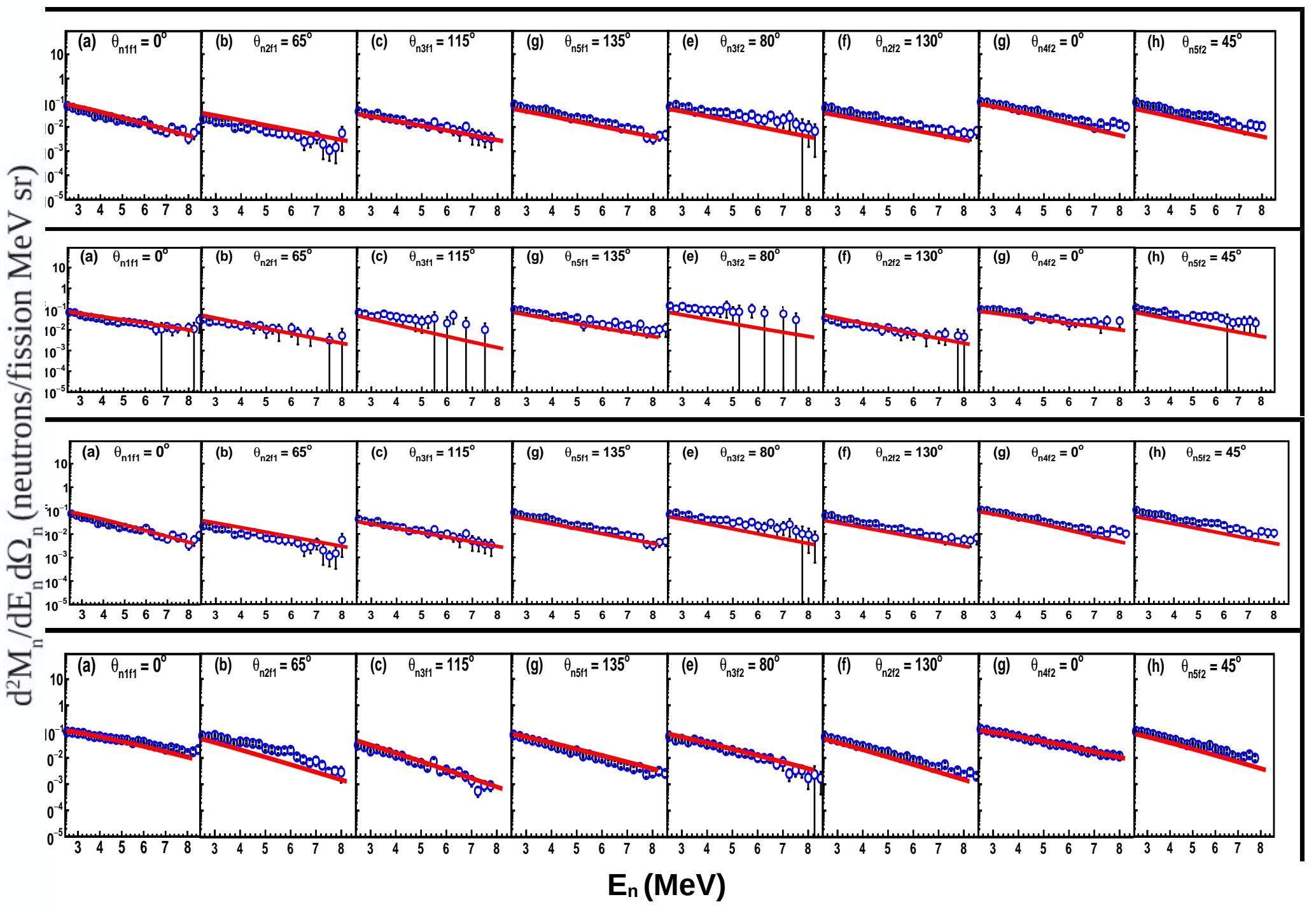
Extraction of v_{pre} and v_{Post}

- A multiple-source least-square fitting procedure followed by a $\chi 2$ minimization procedure was used to extract the pre- and post-scission components (\mathbf{v}_{pre} and \mathbf{v}_{post}) of neutron mutiplicities and temperatures (\mathbf{T}_{pre} and \mathbf{T}_{post}) from the measured neutron energy spectra.
- The Watt expression used for fitting procedure is given as

$$\frac{d^2 M_n}{dE_n d\Omega_n} = \sum_{i=1}^3 \frac{M_n^i \sqrt{E_n}}{2(\pi T_i)^{3/2}} \exp\left[-\frac{E_n - 2\sqrt{\varepsilon_i E_n} \cos \theta_i + \varepsilon_i}{T_i}\right]$$

- Three moving sources of neutrons were considered: neutrons emitted from the CN, which correspond to pre-scission neutron emission (M_{pre}), and neutrons emitted from two fully accelerated fission fragments (FFs), which correspond to post-scission neutron emission (M_{post}).
- Thus, the total neutron multiplicities can be written as the sum

$$\nu_{total} = \nu_{pre} + 2\nu_{post}$$



Double differential neutron multiplicity spectra for the ⁴He + ²³²Th reaction at various excitation energies (from top to botton as 23.93 MeV, 28.85 MeV, 34.75 MeV, 38.68 MeV respectively) for the different neutron detectors.

16/10/2025

Extracted v_{pre} , v_{Post} and v_{Total} (Preliminary)

E _{lab} (MeV)	E*(MeV)	$oldsymbol{\mathcal{U}_{pre}}$	$oldsymbol{\mathcal{U}_{post}}$	VTotal=V _{pre} +2V _{post}
26	20.98	2.30 ± 0.03	0.31±0.032	2.92 ± 0.09
29	23.93	2.17 ± 0.02	0.34 ± 0.05	2.86 ± 0.12
34	28.85	2.69 ± 0.07	0.84 ±0.04	4.38 ± 0.15
40	34.75	2.54 ± 0.06	0.9 ± 0.02	4.34 ± 0.10
44	38.68	2.33 ± 0.06	1.24 ±0.02	4.81 ± 0.10
16/10/2025		Proceedings of the DAE S	Symp. on Nucl. Phys. 68 (2024)	56

SUMMARY

Comprehensive Reaction Studies:

Investigated nuclear reaction dynamics from below to well above the Coulomb barrier, including quasi-elastic scattering, and fusion-fission processes.

Quasi-Elastic Measurements (²⁸Si + ¹⁴⁴Sm):

Extracted barrier distributions to study projectile structure effects; coupled-channel analysis using CCFULL/CCQUEL revealed significant coupling from ²⁸Si excitations.

Fusion-Fission Dynamics (16O + 181Ta, 197Au, 205Tl, 208Pb):

Mass and angular distributions confirm dominant compound nuclear fission at high excitation energies, with evidence of fast-fission contributions.

Neutron Multiplicity Measurements (⁴He + ²³²Th):

Determined pre- and post-scission neutron components to probe nuclear dissipation and extract true dissipation strength (β) for compound fission in ²³⁶U.

Overall Outcome:

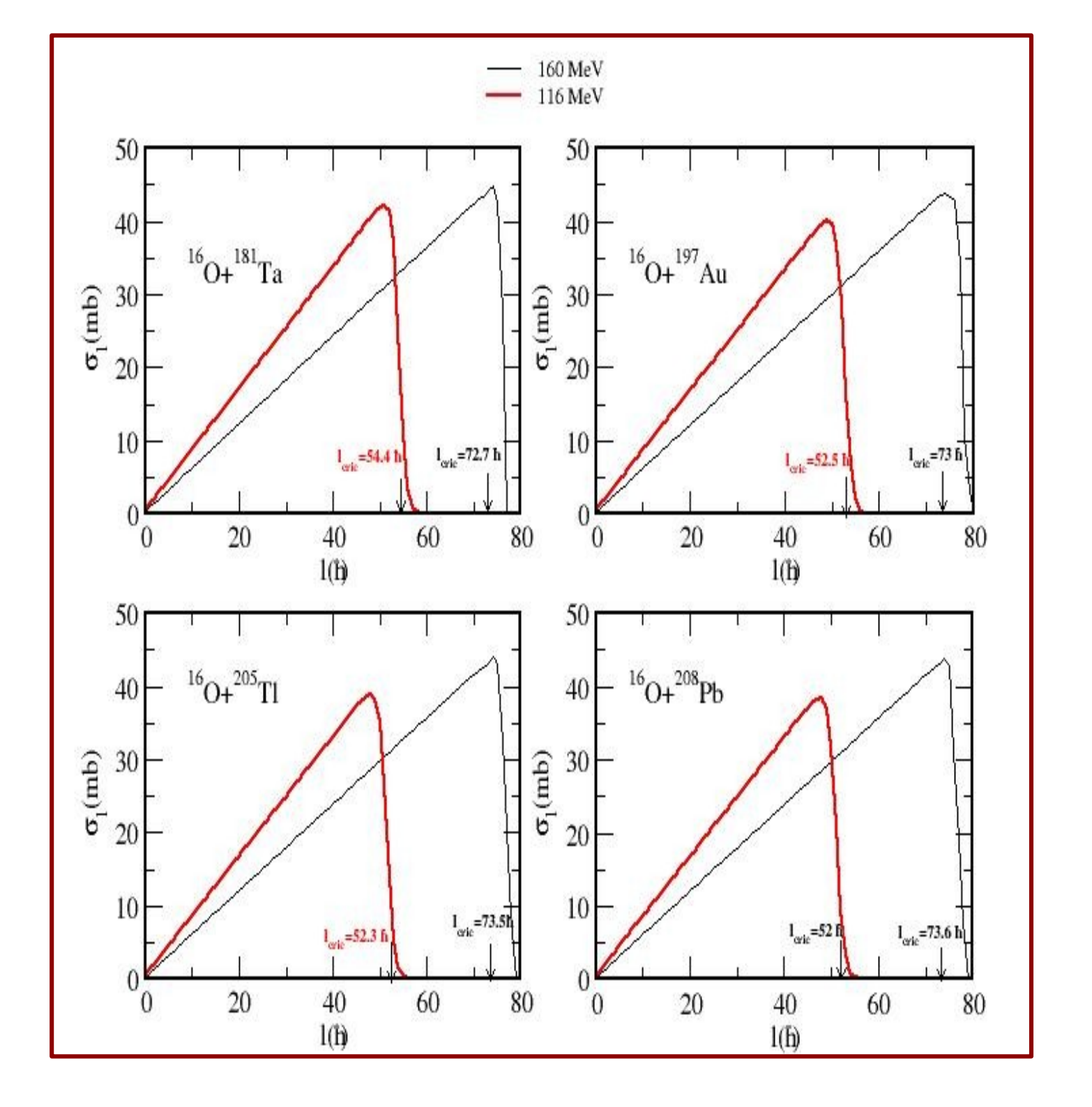
Results bridge reaction dynamics across energy regimes, improving understanding of coupling effects, fission mechanisms, and nuclear dissipation parameters crucial for nuclear structure and astrophysical modeling.

16/10/2025

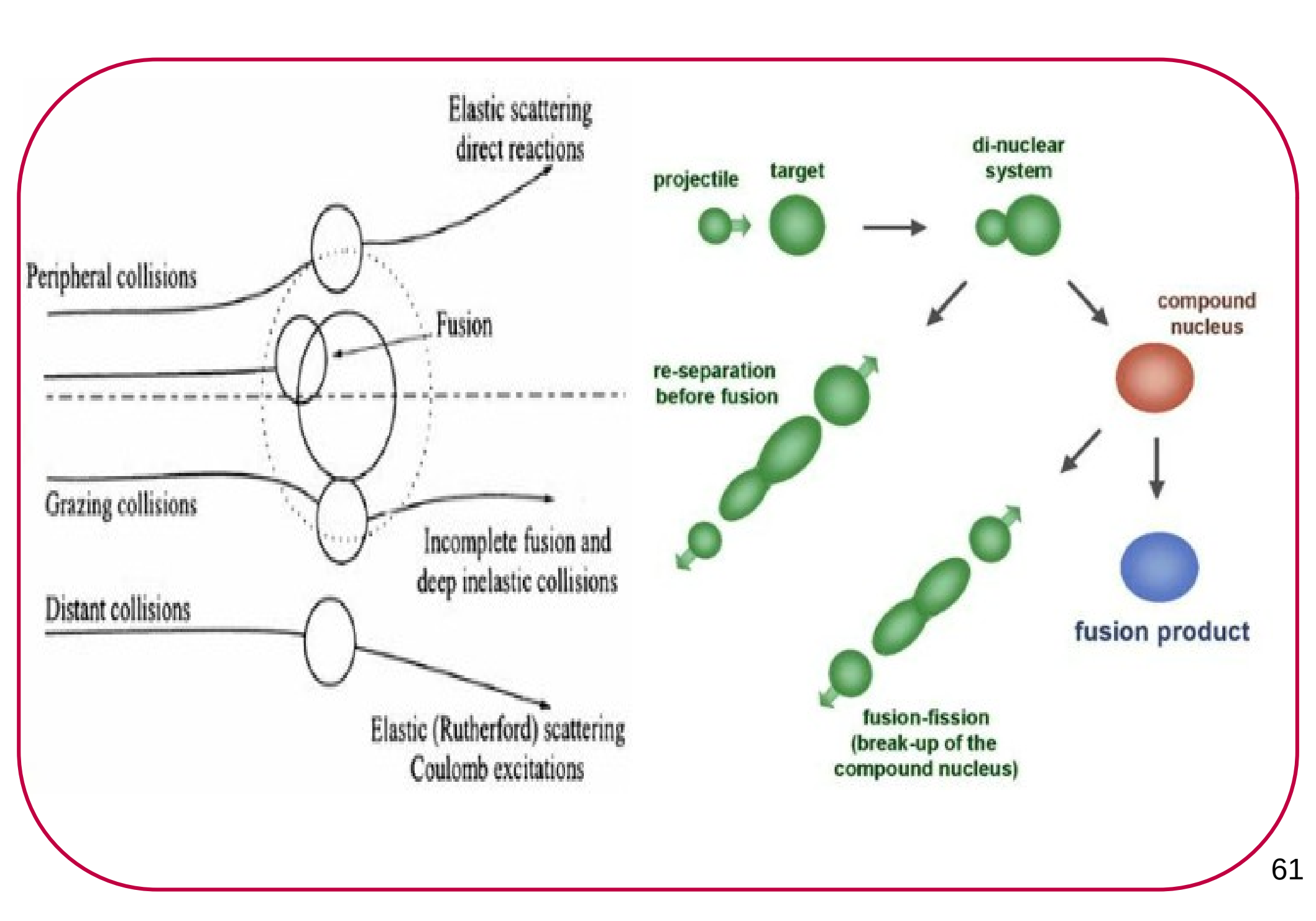


16/10/2025

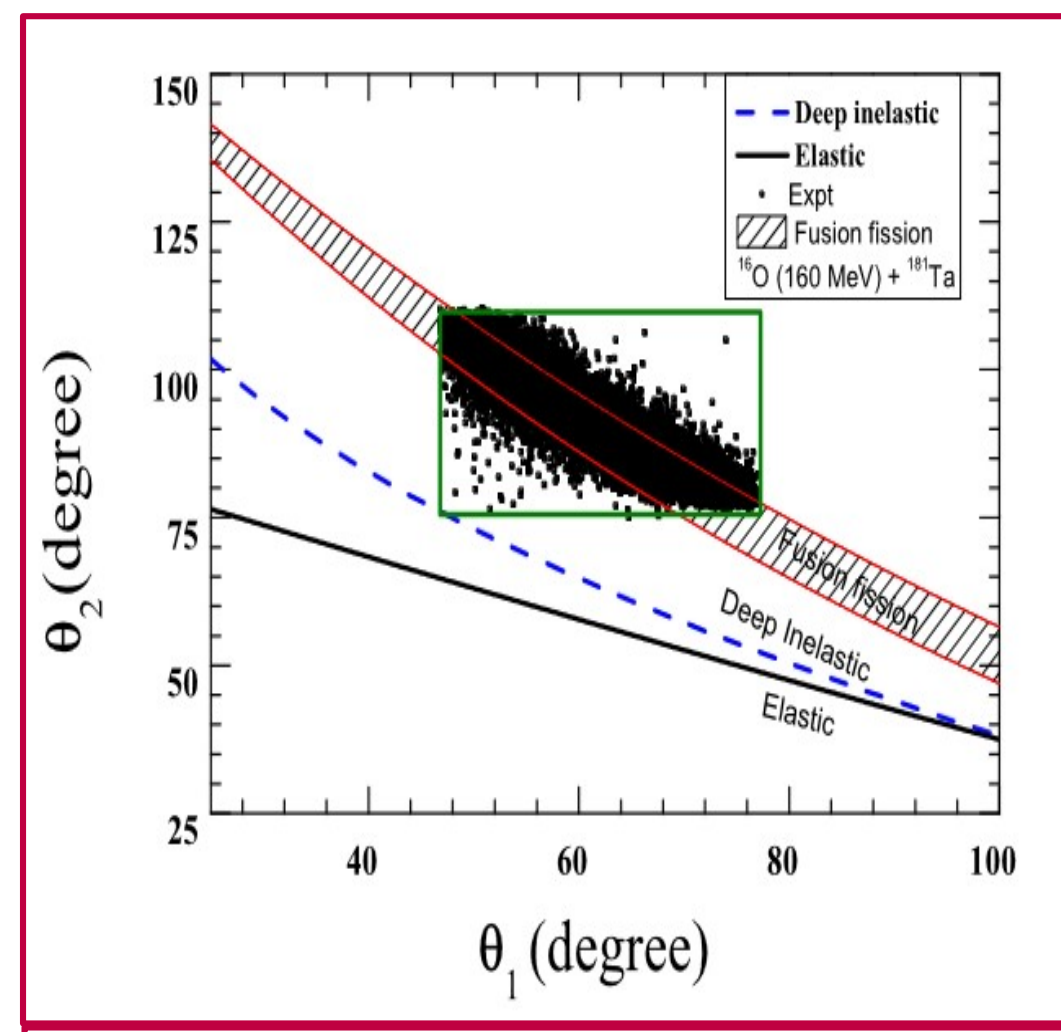
Back up slides



INTRODUCTION:- Nuclear Reactions



DATA ANALYSIS



A representative correlation plot of the simulated polar angle distributions of the events produced in the reaction ^{16}O + ^{181}Ta at the highest beam energy (160 MeV) measured in the experiment. The hatch area indicates that the symmetric fusion fission events are expected to be contained in this region. The elastics events are expected to be below the black line while the deep inelastic events should lie above the dashed blue lines. The detector coverage is shown by the green rectangular box. The measured events are shown by the black dots.

Time of flight difference technique for measurement of mass distribution

$$m_{1} = \frac{(t_{1} - t_{2}) - \delta t_{0} + m_{CN} \frac{d_{2}}{p_{2}}}{\left(\frac{d_{1}}{p_{1}} + \frac{d_{2}}{p_{2}}\right)}$$

$$m_{2} = m_{CN} - m_{1}$$

$$p_{1} = \frac{m_{CN}V_{CN}}{\cos\theta_{1} + \sin\theta_{1}\cot\theta_{2}}$$

$$p_{2} = \frac{p_{1}\sin\theta_{1}}{\sin\theta_{2}}$$